Development of a new inhaled swellable microsphere system for the dual delivery of naringenin-loaded solid lipid nanoparticles and doxofylline for the treatment of asthma

Ashutosh Pareek , Rupal Kothari , Aaushi Pareek , Yashumati Ratan , Pushpa Kashania , Vivek Jain , Philippe Jeandet , Parveen Kumar , Azmat A. Khan , Amer M. Alanazi , Madan Mohan Gupta

PII: S0928-0987(23)00272-5
DOI: https://doi.org/10.1016/j.ejps.2023.106642
Reference: PHASCI 106642

To appear in: *European Journal of Pharmaceutical Sciences*

Received date: 17 April 2023
Revised date: 13 November 2023
Accepted date: 14 November 2023

Please cite this article as: Ashutosh Pareek , Rupal Kothari , Aaushi Pareek , Yashumati Ratan , Pushpa Kashania , Vivek Jain , Philippe Jeandet , Parveen Kumar , Azmat A. Khan , Amer M. Alanazi , Madan Mohan Gupta , Development of a new inhaled swellable microsphere system for the dual delivery of naringenin-loaded solid lipid nanoparticles and doxofylline for the treatment of asthma, *European Journal of Pharmaceutical Sciences* (2023), doi: https://doi.org/10.1016/j.ejps.2023.106642

Development of a new inhaled swellable microsphere system for the dual delivery of naringenin-loaded solid lipid nanoparticles and doxofylline for the treatment of asthma

Ashutosh Pareek [1,*], Rupal Kothari [1], Aaushi Pareek [1], Yashumati Ratan [1], Pushpa Kashania [1], Vivek Jain [2], Philippe Jeandet [3], Parveen Kumar [4], Azmat A. Khan [5], Amer M. Alanazi [5], Madan Mohan Gupta[6]

[1] Department of Pharmacy, Banasthali Vidyapith, Banasthali-304022 Rajasthan, India

[2] Department of Pharmaceutical Sciences, Mohan Lal Sukhadia University, Udaipur, India

[3] Research Unit Induced Resistance and Plant Bioprotection - U.S.C. INRAe 1488, University of Reims, PO Box 1039, 51687 Reims, France

[4] Shri Ram College of Pharmacy, Karnal, Haryana, India

[5] Pharmaceutical Biotechnology Laboratory, Department of Pharmaceutical Chemistry, College of Pharmacy, King Saud University, Riyadh 11451, Saudi Arabia

[6] School of Pharmacy, Faculty of Medical Sciences, The University of the West Indies, St. Augustine, Trinidad & Tobago, WI

*** Corresponding author:**

Ashutosh Pareek, Department of Pharmacy, Banasthali Vidyapith, Banasthali-304022 Rajasthan, India, +919829176631

E-mail: ashu83aadi@gmail.com

Abstract

This study developed a new dual delivery system of naringenin (NRG), a polyphenol, and doxofylline (DOX), a xanthine derivative, as an inhaled microsphere system. In this system, NRG has been first loaded into glyceryl tristearate-based solid lipid nanoparticles (NRG SLN), which were further loaded with DOX into swellable chitosan-tripolyphosphate-based microspheres (NRG SLN DOX sMS). The system was characterised based on particle size, PDI, zeta potential, surface morphology (SEM, AFM, and TEM), solid-state and chemical properties (XRD, IR, and NMR), aerodynamic parameters, drug loading, entrapment efficiency and *in vitro* drug release study. The optimised NRG SLN DOX sMS exhibited particle size, zeta potential, and PDI of 2.1 µm, 31.2 mV, and 0.310, respectively; a drug entrapment efficiency > 79%; a drug loading efficiency > 13%; cumulative drug releases of about 78% for DOX and 72% for NRG after 6 and 12 hours, respectively; good swelling and desirable aerodynamic properties. In addition, *in vivo* studies conducted in mice, a murine model of asthma showed significant reductions in serum bicarbonate and eosinophil counts and improvement in respiratory flow rate, tidal volume, and bronchial wall lining compared with the asthmatic control group. Overall, this novel inhalable dual-delivery system may represent a good alternative for the effective treatment of asthma.

Keywords: Naringenin; Doxofylline; Asthma, Solid Lipid Nanoparticles; Swellable Microspheres; pulmonary drug delivery system

1. Introduction

Asthma, a common, non-contagious, chronic inflammatory disorder of the lower respiratory tract, affects people of all ages and can be life-threatening (Bernstein, 2008). About 300 million people worldwide have asthma, and it is estimated to reach 400 million by 2025 (Li et al., 2019). Due to its complicated aetiology, there is no specific treatment for asthma, although long-term systematic treatments can reduce symptoms and attacks and improve prognosis (Ahmad, 2022). Although pulmonary delivery is the most productive approach, it is challenging due to specific barriers, such as airway structure and defense mechanisms (Ibrahim and Garcia-Contreras, 2013). Currently, inhaled corticosteroids are used effectively with short- and long-acting β-agonists and leukotriene receptor antagonists to treat asthma. However, suffering from systemic side effects such as osteoporosis, adrenocortical suppression, Cushing's syndrome, and the increased risk of infection cannot be ignored (Louie et al., 2013; Liang et al., 2016). Naringenin (NRG) is a polyphenolic flavonoid abundant in citrus fruits and vegetables; it has anti-inflammatory, antifibrogenic, anticancer, and immunomodulatory properties. NRG has shown therapeutic promise in chronic airway conditions such as asthma and chronic obstructive pulmonary disease (COPD) by modulating the expression of cytokines and chemokines, influencing immune cell differentiation, and mitigating lung smooth muscle remodeling (Xue et al., 2019; Chin et al., 2020; Jasemi et al., 2022). However, water solubility and oral bioavailability are poor and should be improved (Chen et al., 2020). Additionally, Doxofylline (DOX) is a next-generation methylxanthine derivative that acts as a bronchodilator and anti-inflammatory and can replace the use of corticosteroids and theophylline but has better tolerability compared to theophylline (Rogliani et al., 2019; Cazzola and Matera, 2020). The study suggests that DOX exhibits a steroid-sparing effect and is effective at notably low doses when co-administered with steroids in both allergic and non-allergic mice, impacting the lungs (Riffo-Vasquez et al., 2018). However, DOX is taken orally three times a day at a dose of 400 mg. Screening the co-delivery of DOX with NRG has not been reported so far. Therefore, there is a need to improve the delivery system and the route of administration to achieve a better therapeutic efficacy of NRG and DOX over a longer period. To this end, the simultaneous targeted delivery of both drugs to the pulmonary region through nanoscale drug delivery systems may be a promising avenue.

Solid lipid nanoparticles (SLNs) possess the synergistic advantages of various carrier systems such as liposomes, niosomes, etc. They can load lipophilic and hydrophilic drugs and exhibit improved physical and chemical stability. In addition, SLNs display rapid absorption, degradation, and sustained release after pulmonary administration. All these properties make SLN particularly suitable for pulmonary delivery (Li et al., 2021).

Particle size is critical for pulmonary drug delivery. Particles must have an aerodynamic diameter of <5 μm to reach the deep lung through the mouth but should not be finer than 0.5 μm to escape exhalation. In addition, Inhaled particles must have a well-established clearance system to remove deposited particles from the lungs (Li et al., 2019). The ciliated epithelial cells of the upper respiratory tract wipe away particles in the throat or mouth. Alveolar macrophages can remove even the particles deposited in the alveolar region through phagocytosis once they get deposited there. Hence, to achieve sustained drug delivery, the microspheres must be designed to reach the lung area and prevent their uptake by macrophages (El-Sherbiny et al., 2010; Li et al., 2021).

Therefore, swellable microspheres represent a promising strategy as they remain within the inhalation size range when dry and expand to larger geometric sizes once in contact with the epithelial lining fluid, thus successfully avoiding macrophage absorption and clearance from the deep lung (El-Sherbiny et al., 2010).

This study developed a novel dual drug administration system that simultaneously delivers NRG and DOX to the pulmonary region, the first time reported for this combination. First, the NRG-loaded glyceryl tristearate-based solid lipid nanoparticles (NRG SLN) were prepared by varying processing parameters and surfactants at different concentrations to achieve a slow and prolonged release effect of NRG in the lungs (Ji et al., 2016; Li et al., 2021). Glyceryl tristearate and soy lecithin were used as lipids and Kolliphor 188 (P188), Poloxamer 407 (P407), and Tween 80 (T80) as surfactants. Furthermore, NRG SLNs and DOX were co-loaded into chitosan-tripolyphosphate-based swellable microspheres (NRG SLN DOX sMS) using the ionic gelation method (Lupascu et al., 2015; Dragostin et al., 2020). Chitosan is a naturally-occurring cationic polysaccharide with a high molecular weight linked by β-1,4-glycoside bonds. It is biodegradable and biocompatible and has been identified as safe in lung epithelial cells and *in vivo* (Kean and Thanou, 2010; Feng and Xia, 2011).

The aim of selecting cationic chitosan and anionic tripolyphosphate (TPP) to manufacture swellable microspheres was to develop loosely cross-linked microspheres that allow rapid release of doxofylline for the treatment of asthma exacerbation as well as the sustained release of naringenin.

The dual drug delivery system, NRG SLN DOX sMS, developed here, was evaluated based on zeta potential, particle size, PDI, entrapment efficiency, drug loading efficiency, swelling index, and surface morphology by SEM, AFM, and TEM Furthermore, solid state and compatibility of the drug were accessed by XRD, IR, and NMR, as well as aerodynamic parameters such as geometric standard deviation (% GSD), fine particle fraction (FPF), and mass mean aerodynamic diameter (MMAD) (determined using an Andersen Cascade Impactor). The *in vitro* drug release study was conducted for 12 hours using simulated lung fluid (SLF). The optimized formulation was screened against an *in vivo* Murine asthma model using egg albumin and trypsin in mice and a histopathological study. Various *in vitro* studies have demonstrated the desired aerodynamic and drug release properties for targeted lung delivery, while *in vivo* studies in mice have revealed the significant efficacy of the developed dual drug delivery system.

2. Materials and Methods

2.1. Materials

Doxofylline was a gift from Suven Pharmaceuticals (India); naringenin (purity- 98%) was purchased from Otto Chemika; chitosan (average molecular weight, 90–310 kDa; deacetylation degree of 75–85%), Kolliphor® P188 (P188), poloxamer 407 (P407), mannitol, lactose, tripolyphosphate (TPP), glyceryl tristearate (GTS), and Tween 80 (T80) were from Merck Sigma Aldrich (India); soy lecithin, trypsin,

and egg albumin were supplied by HI Media Laboratories (India). Dr. Trust's compressor kit was obtained from a local pharmacy. Unless otherwise stated, all additional reagents were of analytical grade and used exactly as procured.

2.2. Preparation of NRG SLN and NRG SLN DOX sMS

2.2.1. Preparation and optimization of SLNs

2.2.1a Preparation Process

NRG SLNs were formulated using the solvent emulsification low-temperature solidification technique with some modifications (Li et al., 2021; Ji et al., 2016). Further, various process parameters such as stirring speed (300-1900 rpm), temperature (60-100° C), and stirring time (1-5 h) of the water phase were optimized along with the effect of the type of the surfactants (P188 and P407) and their concentration (0.5-1.25% w/v) on SLN properties, while keeping NRG (20 mg), Soy lecithin (200 mg), GTS (100 mg) and T80 (1.25 %w/v) as constant. Briefly, the weighed amount of GTS and soy lecithin was mixed and dissolved in 20 ml of absolute ethanol, and NRG was added and completely dissolved in this organic solution at 75 °C and 700 rpm. Further, the specified amount of T80 was dissolved in 60 ml deionised water with constant mechanical stirring (Remi) at 700 rpm. Various other surfactants, such as P188 and P407 (in varying quantities from 0.5 to 1.25% w/v), were also added to the aqueous solution and heated at a specified temperature as per the study design. Then, the oil phase was injected into the water phase to form an emulsion at a constant specific temperature and mechanical stirring (Remi). The biphasic system was maintained at an optimum temperature and speed for a specified period, and the volume of the biphasic system was reduced to about 34 ml to remove ethanol. The resulting biphasic system was rapidly cooled in an ice bath at a temperature of 4°C to obtain an NRG SLN suspension. It was further passed through a membrane filter of 0.45µm size and stored at 4 °C in the refrigerator. The NRG SLN suspension was lyophilised for 24 h using 5%w/v mannitol as a cryoprotectant in a 2:1 NRG SLN to mannitol ratio.

2.2.1b Single-factor optimization

The single factor optimization was carried out using the preparation method "2.2.1a" described above to identify the critical formulation components and process variables that substantially impact SLNs quality attributes, namely zeta potential, polydispersity index (PDI), particle size, and entrapment efficiency. The effect of process parameters like agitation speed, temperature, and agitation time of the water phase was evaluated. In addition, various surfactants at different concentrations were assessed for their effect on SLN quality. The ratio of NRG to lipid (1:5), soy lecithin to GTS (2:1), GTS (100 mg),

and T80 (1.25%w/v) was kept constant throughout the manufacturing process. In addition, a fixed concentration of surfactant P407 of 0.75% w/v was used to optimize the process parameters (Ji et al., 2016; Li et al., 2021).

Effect of the agitation speed of the aqueous phase during injection of the organic phase: the stirring speed was set at five different levels: 300, 700, 1100, 1500, and 1900 rpm, while the temperature was kept constant at 80℃, the agitation time being kept at 2 hours

Effect of temperature during injection of the lipid phase into the aqueous phase: both the agitation speed and the time were kept constant at 1100 rpm and 2 hours, respectively, and the temperature of the aqueous phase was set at five different levels from 60°C to 100°C in 10°C increments. The zeta potential, particle size, PDI, and entrapment efficiency of the prepared NRG SLNs were then compared.

Effect of the stirring time after injecting the organic phase into the water phase: during this study, both the stirring speed and the temperature of the aqueous phase were constantly set at 1100 rpm and 80 °C, respectively, while the stirring time was set at five different steps (1, 2, 3, 4, and 5 hours). The zeta potential, particle size, PDI, and entrapment efficiency of the prepared NRG SLN were then compared.

For process optimization, the effects of the above parameters on quality characteristics such as particle size, zeta potential, PDI, and entrapment efficiency were evaluated with constraints of minimization, maximization (> 30mv), minimization (< 0.3), and maximization, respectively.

Influence of the surfactants and their concentration: after optimizing the process factors, the final formulations were prepared by adjusting the concentration and the type of the surfactant, keeping NRG (20 mg), soy lecithin (200 mg), GTS (100 mg) and T80 (1.25 %w/v) constant. The effect of the different surfactants P188 and P407 was set at four concentrations with GTS ranging from 0.5 to 1.25% w/v. The quality characteristics of SLNs, namely zeta potential, PDI, particle size, drug loading, and entrapment efficiency, were used to optimize the SLNs.

2.2.2 Preparation of NRG SLN DOX sMS

The microspheres loaded with DOX and NRG SLN were prepared using a simple, non-toxic, ionic gelation method (Lupasco et al., 2015; Pai et al., 2016) with the required modifications. The principle behind this is the ionic cross-linking of polycationic chitosan with anionic TPP Briefly, a weighed amount of chitosan was dissolved in 0.1 M acetic acid to prepare a 0.75% chitosan solution and set aside overnight. Then, 100 mg of DOX and NRG SLN powder equivalent to 20 mg of NRG were gradually added to the chitosan solution and mixed at 1000 rpm for 30 minutes using a magnetic stirrer (Remi). Then, the above chitosan solution was injected dropwise into a TPP solution (pH 9.0) of different concentrations using a syringe with an 18-gage needle with gentle stirring. The mixture was kept under constant stirring at 300 rpm for 24 hours to achieve efficient cross-linking or minimal adhesion. The microparticle mixture was separated from the TPP solution and washed thrice with distilled water to remove TPP (Lupasco et al., 2015). The ratio of chitosan to TPP was set at five levels (1:2, 1:4, 1:6,

1:8, and 1:10) to obtain an optimized NRG SLN DOX sMS with desired quality properties. The separated microparticle mixture in distilled water was then freeze-dried (LAB quip) with 5% lactose for 24 hours to obtain the dry microspheres.

2.3 Characterisation of NRG SLNs

2.3.1 Particle size, PDI, and Zeta Potential

Using the Malvern ZetaSizer (Nano-ZS, Biotech USA), measurements of freshly prepared NRG SLN were carried out at 25 °C by diluting 1 ml of the prepared formulation ten times with HPLC-grade water. All the measurements were triplicated.

2.3.2 Entrapment Efficiency (%EE) and Drug Loading (%DL) of the NRG SLNs

By employing centrifugation to separate the unencapsulated drug, % EE was calculated using equation (1). A cooling centrifuge was used to quickly centrifuge 5 ml of the produced SLN suspension for 30 minutes at 18846 *g* (Satari et al., 2020). The supernatant was collected and analyzed using a validated spectrophotometric method at wavelength 282nm (L.A.B. India).

$$\% \text{ EE} = (\text{Total drug added} - \text{Drug in supernatant} / \text{Total drug added}) * 100 \quad (1)$$

To determine the drug loading, SLNs were weighed and centrifuged at 1538 g for 15 minutes after diluting 10 ml of methanol (Wang et al., 2021). A UV-visible spectrophotometer (Lab India) was used to measure the absorbance of the supernatant at wavelength 282nm.

$$\% \text{ DL} = (\text{Weight of the drug in nano/micro-particles} / \text{Weight of nano/micro-particles}) * 100 \quad (2)$$

2.3.3 TEM analysis

Lyophilized NRG SLNs were redispersed in an aqueous solution, and images were captured by tilting the sample at a 60°, using a TEM (JEOL-2100+High Resolution TEM) at 200 kV and a resolution point of 0.194 nm.

2.4 Characterisation of NRG SLN DOX sMS

2.4.1 Particle size, PDI, and Zeta Potential

The prepared NRG SLN DOX sMS were diluted ten times using deionised water. Further, particle size, PDI, and zeta potential were measured by the dynamic light scattering (DLS) technique, and the scattering angle was 90° using the Malvern ZetaSizer (Biotech USA) at 25℃. The measurement was replicated thrice to obtain an average value (Zhang et al., 2018).

2.4.2 % EE and % DL of NRG SLN DOX sMS

For microspheres, 10 mg of lyophilized NRG SLN DOX sMS were dissolved in 20 ml of 0.1 N HCl, centrifuged at 1538 *g* for 15 minutes; the supernatant was then collected, SLF was added to the supernatant, and absorbance was recorded using a UV spectrophotometer at isosbestic points 264 and 284 nm (Lab India) (Gasper et al., 2015). The % EE and % DL were calculated using equations (1) and (2), as mentioned in section '2.3.2'.

2.4.3 Scanning Electron Microscopy (SEM.) Analysis

The surface characteristics of the lyophilized microspheres were determined using a scanning electron microscope (TESCAN Mi80). In order to sputter-coat the samples with gold under vacuum, they were first sprayed onto a copper stub with a double-sided conductive tape adhesive. The photos were taken in the Essence™ software window at an accelerated voltage of 20 kV.

2.4.4 AFM Analysis

Lyophilized sMS were redispersed in distilled water, and a thin film was made on a slide, which was further analysed for 3D surface characteristics using a multimode scanning probe microscope (Bruker Dimension XR).

2.4.5 XRD analysis

Using an X-ray diffractometer (Bruker D8 Advance), the solid-state characteristics of NRG, DOX, dummy SLNs, dummy microspheres (SMs), drug-loaded SLNs, and NRG SLN DOX sMS were observed. The samples were mounted flat, and two scans were performed using Cu-Kα radiation at 40 kV and 40 mA at room temperature with a step size of 0.009°/2 between 10° and 70°.

2.4.6 FTIR spectra

The spectra of both drugs, excipients, the physical mixture (1:1) of free drug and excipients, dummy SLNs, drug-loaded SLNs, dummy sMS, and drug-loaded sMS were recorded by the potassium bromide pellet technique using an FTIR spectrometer (Bruker Vertex V70).

2.4.7 ^{1}H N.M.R. spectra

Spectra of both drugs, dummy SLNs and drug-loaded SLNs, dummy sMS, and drug-loaded sMS were captured using a ^{1}H NMR spectrometer (Bruker Ascend D800). A frequency of 400.13 MHz was used to conduct the experiments, while all samples were dissolved in ^{1}H DMSO.

2.5 Swelling properties

The swelling of chitosan microspheres in SLF (pH 7.4) was gravimetrically quantified by determining their weight changes during swelling, as described by Oliveira *et al.*(Oliveira et al., 2005). 50 mg of SLN-loaded microspheres were weighed and placed in the dialysis bag, then in the SLF medium. The SLF medium was continuously stirred with a magnetic stirrer (Remi) at 50 rpm and at different predetermined time points ranging from 0 to 120 min. The dialysis bag was removed, and the swollen microspheres were gravimetrically weighed. The degree of swelling (%) was calculated using Equation 3, and a plot was made between the time and the degree of swelling (Oliveira et al., 2005).

Degree of swelling (%) = (W1 - W2)/W2 × 100 ----- (3)

Where: W1 - the weight of swollen microspheres; W2 - the weight of dried microspheres

2.6* In vitro *lung Deposition Studies

The theoretical mean aerodynamic mass diameter (Dt) was determined according to the tapped density measurement (Zhang et al., 2018).

An eight-stage Andersen cascade impactor (ACI) (Westech Scientific) was used to assess actual aerodynamic diameter and aerosol output. The ACI consists of an intake, a pre-separator, seven stages, and a final filter. The pre-separator was coupled to the impactor to prevent aggregation of particles of larger size. The ACI stages were assembled and connected to a vacuum pump with a flow meter. The airflow was then set to 60 l/min. Powders containing 100 mg of the NRG + DOX mixture and the lyophilized microspheres were placed in capsules (size 2) and added to the apparatus. The capsules were placed in a Rotahaler apparatus (Cipla Ltd., India) and inserted into a rubber mouthpiece moulded and attached to a glass neckpiece of an endoscope operated at 60, 90 l/min. The mass median aerodynamic diameter (MMAD), percentage geometric standard deviation (%GSD), and percentage fine particle fraction (%FPF) were determined (Zhang et al., 2018).

2.7 In vitro Drug Release Studies

The drug release study was performed in SLF using the dialysis membrane method with the necessary modifications (Chen et al., 2021). Briefly, a dialysis bag (high medium: dialysis membrane-110) was loaded with 10 mg of the lyophilized NRG SLN DOX sMS dispersed in 1 ml of SLF (pH 7.4) and stirred at 100 rpm and 37.5 °C in an orbital shaker in the incubator while suspended in 150 ml of SLF containing 0.8% Tween 80 (v/v). An aliquot of 2 ml was withdrawn after 0.25, 0.5, 1, 2, 4, 6, 8, 9, 10, 11, and 12 hours and passed through a 0.22-μ membrane filter; the equal volume of fresh SLF was then added to

maintain the sink condition. The amount of drug release was calculated using a UV spectrophotometer at wavelengths 284nm and 264nm for naringenin and doxofylline, respectively. The percent cumulative release of NRG and DOX was calculated at each time point, and the release data were fitted to various kinetic release models, namely zero order, first order, Higuchi, and Korsmeyer-Peppas to assess the best-fit release kinetics model based on the linearity of the release curves. In addition, the possible release mechanism was predicted by the value of “n” of the Korsmeyer-Peppas equation (Pai et al., 2016; Chen et al., 2021).

2.8 In vivo Studies

2.8.1 Murine Asthma Model Using Egg Albumin and Trypsin

The study protocol was previously approved (BV/IAEC/2022/94) by the IAEC of Banasthali Vidyapith, and all CPCSEA guidelines were followed for all experiments. In addition, healthy male Swiss albino mice (n=24) weighing from 25 to 30 g were included in the study. Animals were housed in polypropylene cages with unrestricted access to food and water on a 12-hour light-dark cycle at 25±1°C and 50±15% RH. As previously reported by Gohil et al., trypsin and egg albumin were combined to induce asthma in mice (Gohil et al., 2011). For the study design, four groups were formed with six animals in each group: Group I (normal control), Group II (asthma), Group III (asthma + dexamethasone), and Group IV (asthma + optimized NRG SLN DOX sMS). All animal groups except the normal control group were exposed to trypsin aerosol (1 mg/ml and 1 ml/min) once daily for 5 minutes and rested for 2 hours before exposure to egg albumin (1% w/v solution and 1 ml/min). The process was repeated for ten days when the egg-albumin aerosol was discontinued, while trypsin exposure continued until day 21. Group I animals received no treatment except saline. The animals in group II were irradiated with egg albumin but received no drug treatment. In groups III and IV, the animals received dexamethasone (5mg/kg, p.o.) and optimized NRG SLN DOX sMS (300mg/kg, dry powder via inhalation), respectively, from day 22 to 35. Egg albumin was administered 2 hours after the last treatment dose on day 35.
Lung function (respiratory rate, airflow rate, respiratory volume) and serum bicarbonate levels were measured in each animal on day one before any exposure (baseline), day 21 after trypsin exposure, and day 35 after egg albumin exposure. In addition, bronchoalveolar lavage (BAL) and histamine content in lung tissue homogenates were measured on day 35, and lung tissue histopathology was performed (Gohil et al., 2011).

2.8.2 Measurement of airway hyperresponsiveness/lung function

Head-out body plethysmography was used to measure airway hyperresponsiveness (Glaab and Braun, 2021). Briefly, the head of each animal was inserted through the cervical collar into a ventilated head exposure chamber, and the animals were then placed in a chamber with vitreous plethysmographs. The respiratory rate, airflow rate, and tidal volume were measured using a pneumotachograph attached to the pressure transducer (Glaab and Braun, 2021).

2.8.3 Measurement of Serum Bicarbonate

Shah et al., 2010 described a method that determined serum bicarbonate levels using the colorimetric titration method. Briefly, serum was separated from the collected blood (2 ml), mixed with saline, and titrated against 0.1 N NaOH using phenol red as an indicator. The NaOH consumed was noted, and serum bicarbonate was calculated (Shah et al., 2010).

2.8.4 Isolation of B.A.L. Fluid

Using 24-gauge catheters, 1 ml of PBS was perfused 2-3 times into the trachea, and the BAL fluid was collected on day 35, 3 hours after egg albumin provocation, or just before the animal died, whichever came first (Oh et al., 2011). The total number of inflammatory cells was counted using a hemacytometer (Drew Scientific Hemavet 950). The differential leukocyte count was determined according to the procedure described by Gohil et al. (Gohil et al., 2011). Briefly, the BAL fluid collected above was centrifuged at 2000 rpm for 5 minutes, the pellet was resuspended in saline, and slides were prepared using the Giemsa staining kit and viewed under the microscope.

2.8.5 Release of Histamine from Lung Tissues

Animals were sacrificed on day 35, 3.5 hours after egg-albumin provocation or shortly before death, and their lungs were excised and dissected into fragments. The dissected lung tissue was placed in tubes containing 2 ml of chilled calcium-free Tyrode solution and refrigerated until usage. Lung tissue (200 mg wet weight) was added to the test tubes. Then, 1.8 mmol L^{-1} calcium chloride was added to the test tubes and incubated at 37 °C for 10 minutes. The lung tissue was then incubated with 2 mg L^{-1} egg albumin for 15 minutes at 37 °C. The reaction was stopped after 15 minutes by filtering the medium through a nylon mesh (100 mm). The histamine content in the medium was measured fluorimetrically (Cais, 1961; Gohil et al., 2011).

2.8.6 Histopathology of the lungs

After removing the right lungs of mice, which had not been lavaged, they were fixed in formalin (10% v/v) for 48 hours. These have been further treated with different alcohol gradients and embedded in paraffin. It was then sliced into 5 µm fine sections and stained with hematoxylin and eosin. The infiltrate of inflammatory cells and the wall was examined by light microscopy at 400× magnification, as described previously (Oh et al., 2011; Zhang et al., 2018).

2.9 Statistical Analysis

The data obtained from various *in vitro* and *in vivo* analyses were represented as mean±standard deviation (SD) (n=3) and mean±standard error of the means (SEM) (n=6), respectively. The statistical significance of the obtained results was analyzed by analysis of variance (one-way ANOVA) followed by post hoc Tukey's multiple range tests using GraphPad Prism 9. Values of * $P < 0.05$, ** $P < 0.01$, *** $P < 0.001$ were considered significance levels wherever necessary.

3. Results and Discussion

In this study, the dual drug release system NRG SLN DOX sMS was prepared to deliver NRG and DOX to the lung tissue in one step with a two-step release behavior. This newly designed pulmonary approach with desired aerodynamic properties allows for the rapid release of DOX from a swellable microsphere matrix and a more controlled release of NRG by SLNs followed by microsphere matrix, which may improve local availability in lung tissue and thus the efficacy of both drugs with a better therapeutic profile and better patient compliance.

3.1. Preparation and optimization of SLNs

The NRG SLNs were successfully prepared by solvent emulsification with low-temperature solidification, a reliable, standardized, and reproducible method for preparing SLNs. The process parameters, such as stirring speed, temperature, and stirring time of the aqueous phase, were optimized using single-factor optimization. In addition, the effects of different surfactants (P188 and P407) at different concentrations on the quality properties of SLNs, namely zeta potential, PDI, particle size, and entrapment efficiency, were investigated, and the following results were obtained.

3.1.1. Single-factor Optimization

3.1.1a Impact of Water Phase Stirring Speed

The lipids dissolved in absolute ethanol must be dispersed by the mechanical force generated by the stirring speed, and the dispersed oil globules were introduced into the water phase to be stabilized by surfactants during the preparation process of SLNs (Li et al., 2021). In addition, it was desirable to continuously stir the aqueous phase at high speed to obtain a stable and homogeneous thermal emulsion system (Moribe et al., 2012). Therefore, the stirring speed while injecting the organic phase was a critical parameter for the quality of the SLNs. The results are listed in Table 1.

[Please insert Table 1 here]

Table 1 shows that the stirring speed substantially affected the particle size, polydispersity index, and entrapment efficiency of SLNs, while slightly affecting zeta potential. The prepared SLNsdisplayed greater particle size and polydispersity index at slow speeds, likely due to uneven mixing of the lipid phase with the water phase, resulting in a less stable system and hence an emulsion. When stirred too quickly, the size and PDI of SLNs remained higher, possibly due to the destruction of particle morphology and the formation of more foam, affecting the surfactants' emulsifying effect. The results are in

agreement with others (Ji et al. 2016; Li et al. 2021), which reported an increase in particle size and wide distribution of SLNs produced at higher and lower stirring speeds.

However, the dependence between particle size and zeta potential was also observed at different speeds. The entrapment efficiency was highest at a stirring speed of 1100 rpm, and the particle size and PDI were also small as desired, so we consider it to be the stirring speed optimal for further preparations.

3.1.1b Effect of temperature during injection of the organic phase into the water phase

For the preparation of adequate SLNs, the solid lipids must be in a completely liquid state by an appropriate temperature so that they can be transformed into small droplets of the oil phase during the emulsification of the system by mechanical stirring under the action of surfactants, which convert into SLNs upon cooling. Therefore, when injecting the organic phase, the temperature of the aqueous phase was a critical parameter for the quality of SLNs. This study investigated the effects of different temperature conditions on the quality characteristics of SLNs (see Table 2).

[Please insert Table 2 here]

Table 2 shows that, at temperatures below 80 °C, the particle size and the dispersity index of the prepared SLNswere higher, while at temperatures above 80 °C, the particle size remained similar, but the PDI increased variably, which is consistent with the previous studies (Li et al., 2021). This was due to the fact that the lipid component can harden at low temperatures, preventing it from being in a liquid state throughout the preparation process and making the particle size of the obtained SLNs too large, which is not favorable to emulsification. Moreover, at low temperatures, the interaction between the surfactant, water, and oil particles was negligible due to the solidification of the lipid material. When the temperature increases (60-80 °C), the lipid component can be emulsified into liquid oil droplets, resulting in particles of smaller size and a narrower particle size distribution in the prepared SLNs. Too high a temperature (90 and 100 °C) leads to a broadening of the SLNs' particle size distribution rather than condensation. If the temperature of the system is too high, the kinetic energy of the particle will increase as the SLNs solidify, causing them to aggregate and take an irregular shape.

In addition, it was found that the entrapment efficiency of the prepared SLNs was quite similar (89-92.7%) at 60-80 °C and decreased at very high temperatures (90 and 100 °C), probably because the surfactant molecules had much higher kinetic energy than surfactants-water-lipids interactions at very high temperatures, resulting in the formation of disfigured globules with low entrapment efficiency. The interactions between the particles and the surfactant molecules dominate the thermal fluctuations only for a moderate temperature range, allowing the particles to diffuse over a certain distance (Yuan et al., 2003). A temperature of 80℃ was therefore selected.

3.1.1c Effect of stirring duration after introduction of the lipid phase to the aqueous phase

The formation of emulsion droplets usually occurs immediately when the lipid phase is introduced into the aqueous phase. A longer time is required for sufficient adsorption of the surfactant at the interface to stabilize the lipid phase globules against coalescence since the surfactant molecules have already reached the surface of the oil droplets (Major-Godlewska, 2020). In this study, the effects of different stirring times (1-5h) of the water phase after injection of the organic phase to form an emulsion on the quality characteristics of SLNs were investigated; the results are shown in Table 3.

Table 3 shows that for a short stirring time (1 h), the PDI, particle size, and percentage EE of the prepared SLNs were large, high, and relatively low, respectively. Large particle size and wide distribution of SLNs for a short stirring time could be inefficient in producing a stable final emulsion and, thus, flocculation. When the stirring time was set at 2 hours, the particle size, dispersity, and percentage EE were small, narrow, and relatively high. However, no significant changes in particle size and EE were observed after further increasing the stirring time. The zeta potential slightly decreased with increasing stirring times. Taking into account the particle size and EE, we considered that a stirring time of 2 hours was sufficient after the injection of the organic phase for the subsequent preparation of SLNs.

[Please enter Table 3 here]

3.1.1d Influence of Surfactant Concentration

An adequate concentration of surfactant is necessary to ensure stability and narrow the size distribution of the nanoparticles. Excessive use of a surfactant may decrease SLNs' loading capacity. The effect of the type of surfactant and their concentration was studied, keeping the Tween 80 concentration constant (0.75% w/v) (Table 4).

Particle size, PDI, and Zeta Potential

An increase in the concentrations of P188 (0.5 to 0.75% w/v) and P407 (0.5 to 1% w/v) resulted in a dramatic decrease in the particle size of the prepared SLNs. It decreased from 311.3 to 159 nm and from 429.2 to 178.9 nm in the case of P188 and P407, respectively. This could be due to the fact that the nanoparticles are not sufficiently coated with surfactants at lower concentrations, resulting in less stabilisation of the particle dispersion (Rehfeld, 1967; Helgason et al., 2009; Kushwaha et al., 2013; Guttoff et al., 2015; Chuacharoen et al., 2019). By increasing the concentration of P188 from 0.75% to 1.25%, no significant change in particle size was observed up to 1%. A slight increase in the particle size of SLNs was observed at a concentration of 1.25%. This may be because, at a higher concentration, the reduction in the diffusion rate of the solute molecules leads to an increase in the outer phase's viscosity, which could be responsible for the shift in particle size.

A further increase in the concentration of P407 from 1 to 1.25 %w/w led to a similar increase in particle size as for P188. It could also be because increasing the poloxamer concentration led to flocculation due to the dehydration of the poloxamer chains and a decreased steric stabilisation efficiency. These results are in agreement with the observation of Pandita et al. (Pandita et al., 2009) with one minor difference. Pandita et al. (Pandita et al., 2009) previously reported that increasing the poloxamer concentration to 1.5% decreases the particle size, but increasing it to 2% further causes aggregation of SLN particles. This difference could be due to the T80 surfactant used in the study at a concentration of 0.75% (w/w), which synergizes the emulsifying effect via SLN formation. In addition, Muller et al. (Müller et al., 2002) previously found that increasing the poloxamer concentration to 1% resulted in a decrease in the size of SLN. In the present work, 0.75% P188 and 1% P407 were sufficient to cover the nanoparticle surfaces and avoid aggregation. In agreement with a previous work by Steiner et al. (Steiner and Bunjes, 2021), the particle size of SLNs was significantly smaller when P188 was used rather than P407.

Increasing the concentration of P407 decreased the PDI of the produced SLNs. Whereas in the case of P188, the PDI was decreased to 0.172 up to a concentration of 0.75% of the surfactant. A further increase in the concentration of P188 resulted in a minimal increase in the PDI. Increasing the surfactant concentration may decrease interfacial tension and increase emulsification to some extent, leading to a lower PDI of the SLNs (Rehfeld, 1967; Guttoff et al., 2015; Chuacharoen et al., 2019). A further increase in surfactant concentration may lead to particle aggregation. Overall, the formulations behave like monodisperse suspensions as long as the PDI is less than 0.3, except for the F1 formulation.

The zeta potential is often essential for understanding the stability of a colloidal dispersion. It is currently recognized that more than 30 mV zeta potentials are required for complete electrostatic stabilization (Thatipamula et al., 2011). As indicated in Table 4, the absolute value of the zeta potential indicated the stability of all formulations except F1.

Determination of % DL and % EE.

Table 4 shows that the % EE of the prepared SLNs ranged from 82.77 to 92.06% and 85.35 to 95.5% for P407 and P188, respectively. Moreover, it was found that the % DL ranged from 11.51 to 17.65% and 14.71 to 19.42% for SLNs prepared with P407 and P188, respectively.

It was observed that increasing the surfactant concentration resulted in a slight increase in % EE and % DL for P407 and P188, respectively, which was attributed to the enhancement of the surface coverage of the nanoparticles that prevented the drug from escaping from the lipid matrix (Kushwaha et al., 2013). Moreover, increasing the surfactant concentration improved the solubilization of the drug during the process, which tended to increase % EE (Guttoff et al., 2015). These results agree with the findings of a previous study by Pandita et al. (Pandita et al., 2009). However, at a higher concentration of P188 (1.25%), a slight to moderate decrease in entrapment efficiency and drug loading was observed. It is

likely because, at higher concentrations, the surfactant promotes aggregate formation and flocculation, which reduces the amount of drug available for entrapment, resulting in lower tangle and drug loading. Moreover, the drug could be lost due to binding to some additional poloxamer molecules during SLN formation (Pandita et al., 2009).

[Please enter Table 4 here]

After considering the selected quality attributes and the desired threshold, formulation F6 was selected as the optimized formulation and incorporated into DOX-containing chitosan microspheres. Formulation F6, which contained the surfactants P188 (0.75%) and T80 (0.75%), exhibited small particle size (< 160 nm), homogeneous monodisperse suspension (PDI around 0.170), excellent stability (zeta potential > 40 mV), higher entrapment efficiency (95.4%), as well as higher drug loading (19.4%). (See Table 4 and Figure 1)

[Please insert Figure 1 here]

Figure 1: Graphical representation of a) Particle size and polydispersity index of optimized SLNs; formulation F6 contains 0.75% P188 b) Zeta potential of optimized SLNs; formulation F6 contains 0.75% P188. Abbreviations: SLNs, solid lipid nanoparticles; P188, Kolliphor P188.

3.1.2 TEM Analysis

The morphology of drug-loaded SLNs was studied by T.E.M. SLNs had a smooth surface and a spherical form, with particle sizes ranging between 100 to 200 nm (Figure 2). The average particle size of SLNs was 124.3±15.43 nm (mean ± standard deviations, n=10). The SLNs had a slightly smaller diameter than the hydrodynamic diameter determined by the zeta-sizer.

[Please insert Figure 2 here]

Figure 2: Transmission electron microscopic image of optimized SLNs, formulation F6 contains 0.75% P188. Abbreviations: SLNs, solid lipid nanoparticles; P188, Kolliphor P188.

The obtained size was slightly less than the zeta sizer result, showing the presence of a hydrodynamic layer over the SLN particles. The poloxamer provided SLNs with a smooth surface with few or no pores, resulting in decreased drug loss during production, hence a high entrapment efficiency.

3.2 Preparation of NRG SLN DOX sMS

Various processes involving cross-linking chemicals such as sodium hydroxide, glutaraldehyde, and formaldehyde are used to prepare chitosan microparticles. These are associated with toxicity and various undesirable side effects that can be avoided through ionic cross-linking with TPP. Due to its non-toxic and anionic nature, TPP is an excellent alternative to strong cross-linking agents such as formaldehyde (Agnihotri et al., 2004; Gupta and Jabrail, 2006). The polycationic chitosan, which in an acidic medium protonates the NH_2 group to NH_3^+, ionically interacts with the negatively charged counterion of TPP during ionic gelation to form a matrix (Lupascu et al., 2015). Reportedly, this interaction between chitosan and TPP affects the fabricated microparticles' surface shape, particle size, and release profile. In addition, changing the chitosan: TPP ratio affects drug entrapment, drug release profile, and microparticle size (Agnihotri et al., 2004). Moreover, the cationic structure of chitosan gives it mucoadhesive qualities, allowing it to bind to the pulmonary mucosa and delay drug elimination (Pai et al., 2016).
In this study, we maintained the TPP solution at a pH of 9.0; at this pH, both hydroxyl and phosphorus ions are present and can interact with the NH_3^+ groups of chitosan. Different ratios of chitosan to TPP were used to produce stable chitosan microparticles with variable swelling properties.

3.3 Characterisation of NRG SLN DOX sMS

Physically stable microspheres loaded with NRG SLN and DOX were successfully prepared. The ratio of chitosan to TPP played an important role in the entrapment efficiency, particle size, stability, size distribution, and drug release of the chitosan microspheres. It was varied in different ratios (1:2, 1:4, 1:6, 1:8, and 1:10) to obtain microparticles with desired attributes for pulmonary delivery.

3.3.1 Particle size, PDI, and Zeta Potential

As shown in Table 5, the particle size of the prepared NRG SLNs and DOX-loaded microspheres was increased from 0.59 to 2.41 µm by decreasing the molar ratio of chitosan to TPP These results are consistent with several previous studies (Desai and Park, 2005; Cho et al., 2014; Buzia et al., 2015; Pai et al., 2016; Debnath et al., 2018), which reported an increase in the particle size of microparticles with an increase in the amount of the added cross-linking agent. This could be because a higher concentration of TPP produces highly viscous dispersion and large droplet size during ionic gelation (Pai et al., 2016). All batches had particle sizes below 5 µm, which is essential for administration by inhalation. A respirable fraction is the proportion of inhaled particles that can reach the alveolar areas of the lungs. Particles less than 5 µm are considered respirable.
The PDI of the prepared formulations was less than 0.6, and a slight decrease in the dispersity index was observed with increasing TPP contents, but an increase in PDI was observed at a very high TPP: chitosan ratio (Table 5). This increase in PDI could be due to the formation of aggregates at very high concentrations. The particle size exhibited a unimodal distribution, which was also evident from the low polydispersity indices (Figure 3a)

In addition, all NRG SLN and DOX microspheres exhibited a positive zeta potential, ranging from 29 to 34 mV, with an average of 32.2 ± 2.83 mV (Table 5, Figure 3b). The zeta potential value was decreased by increasing the negative charge of TPP. These results are consistent with other findings (Debnath et al., 2018).

[Please enter Table 5 here]

[Please enter Figure 3 here]

Figure 3: Graphical representation of a) the particle size of optimized microspheres, MS3 b) the Zeta potential of the optimized microspheres, MS3.

3.3.2 Determination of % DL and %EE

The data in Table 5 show that the entrapment efficiency ranged from 63.6 to 85.4%, while the drug loading ranged from 10.8 to 17.4%. Both the % EE and the % DL decreased with increasing TPP contents. These results are in agreement with previous findings (Buzia et al., 2015; Pai et al., 2016; Debnath et al., 2018). At low TPP fraction, the chitosan microparticles remained in a loose network, which allows for a higher hydrodynamic free volume and thus offers a greater chance for accommodating the drug solution in the matrix, while at high concentrations of TPP, the chitosan network became denser and led to low drug entrapment. Thus, increasing the anionic TPP concentration increased the emulsion globules' size, and ionic gelation negatively affected co-loading with DOX and NRG SLNs. However, these results contradict the findings of another study (Mulia et al., 2018), where a decrease followed by an increase in the percentage of % EE and % DL were described when the TPP concentration was increased from 2 to 8%.

3.3.3 Scanning Electron Microscopy (SEM.)

The SEM image in Figure 4 shows that the shape of the sMS was slightly asymmetrical, and the surface was rough, which could be due to loose cross-linking between the chitosan molecules. The combination of chitosan, lactose, NRG-SLNs, and the DOX may lead to complex interactions and could be the possible reason for slight deformity in the shape of the lyophilized dry microparticles. Slight aggregation of SLNs during the freeze drying could also affect the shape. In addition, the presence of drug particles on the surface and the use of lactose during freeze-drying were responsible for the roughness and the complex structure of the prepared microspheres. The microspheres had a slightly smaller diameter than the hydrodynamic diameter determined by the zeta-sizer.

[Please enter Figure 4 here]

Figure 4: Scanning electron microscopic images of optimized NRG SLNs and DOX-loaded microspheres. Abbreviations: NRG SLNs, Naringenin-loaded solid lipid nanoparticles; DOX, Doxofylline.

3.3.4 Atomic Force Microscopy (AFM.)

The morphology of the fabricated microspheres was also analyzed using AFM images. As seen in Figure 5, the prepared microspheres exhibited a narrow particle size distribution, a rough surface, and a slightly irregular shape, similar to the images obtained from SEM.

[Please enter Figure 5 here]

Figure 5: Atomic force microscopic images of the optimized microspheres, MS3.

3.4 X-ray diffraction (XRD) Analysis

The X-ray diffraction patterns show the crystalline nature of DOX and NRG, and the sharp diffraction peaks can be seen in Figure 6. However, the less pronounced peaks in the case of drug-loaded SLNs and sMS indicate an amorphous solid state of both drugs and proper encapsulation of the drug in the nanoparticles and the microspheres. In the case of NRG SLN DOX sMS, the insignificant peak of NRG SLNs indicated the significant entrapment of the nanoparticles in the microspheres.

[Please enter Figure 6 here]

Figure 6: X-ray diffraction (XRD) graphs of NRG, DOX, NRG SLNs, Dummy SLNs, Dummy sMS and NRG SLN DOX sMS. Abbreviations: NRG, Naringenin; DOX, Doxofylline; NRG SLNs, Naringenin loaded solid lipid nanoparticles; Dummy SLNs, Dummy solid lipid nanoparticles; Dummy sMS, Dummy microspheres; NRG SLN DOX sMS, Naringenin solid lipid nanoparticles and Doxofylline co-loaded microspheres.

3.5 FTIR Spectroscopy

As shown in Figure 7, the characteristic functional groups of naringenin were found to be the same in the physical mixture, indicating compatibility between the selected lipids and NRG. In addition, no distinct peaks of NRG were observed in the spectra of NRG-SLNs, indicating that NRG was successfully entrapped in SLNs. The characteristic peaks of dummy SLNs, NRG SLNs, were all the same, indicating that the presence or absence of NRG did not affect the FTIR findings of SLNs, once again demonstrating that NRG was correctly included in SLNs. The functional groups of DOX were also unmodified in the case of sMS and the physical mixture, showing no interactions. However, none of the characteristic DOX peaks were observed in the sMS spectra, suggesting that DOX might have been effectively entrapped in the microspheres.

[Please enter Figure 7 here]

Figure 7: FTIR characterization spectra of (A) NRG, Physical Mixture, Excipients, Dummy and Drug Loaded SLNs (B) DOX, Physical Mixture, Excipient, Dummy and Drug loaded sMS. Abbreviations: FTIR, Fourier transform infrared spectroscopy; NRG, Naringenin; DOX, Doxofylline; SLNs, Solid lipid nanoparticles; sMS, Microspheres.

3.6 1H N.M.R. Spectroscopy

Similar results were obtained with NMR spectroscopy (Figure 8). Even though the NMR spectrum did not reveal much information about these samples, the absence of typical peaks for NRG in the spectra of NRG-SLNs and of peaks for DOX in sMS provided further evidence that NRG and DOX were well entrapped in the carriers.

[Please enter Figure 8 about here]

Figure 8: Nuclear magnetic resonance characterization spectra of A) NRG B) Dummy SLNs C) NRG-loaded SLNs D) DOX E) Dummy sMS F) NRG SLN DOX sMS. Abbreviations: NRG, Naringenin; Dummy SLNs, Dummy solid lipid nanoparticles; NRG SLNs,- Naringenin-loaded solid lipid nanoparticles; DOX, Doxofylline; Dummy sMS, Dummy microspheres; NRG SLN DOX sMS, Naringenin solid lipid nanoparticles and Doxofylline co-loaded microspheres.

3.7 Swelling properties

Since the ideal size range of 1 to 5 µm is expected to ensure effective deposition in the lung despite being the most susceptible to macrophages, a robust swelling index is required to prevent macrophage uptake. The swelling characteristics of the prepared microspheres are shown in Figure 9. The swelling index decreased from 102±3.1 to 52±2.7% in 2 hours with an increase of the TPP/chitosan ratio (2:1 to 10:1) due to the improved cross-linking of the chitosan matrix with an increase of the anionic TPP fraction. The results indicated that the loose cross-linking of the matrix caused swelling of the microspheres, leading to the required size increase. Within 15 minutes, the swelling index of the optimized formulation MS3 reached 63±1.3%, further indicating the ability of the microspheres to prevent uptake by alveolar macrophages.

[Please enter Figure 9 about here]

Figure 9: Comparative graphical representation of the swelling Indexes of different formulations of microspheres. Values are represented as mean ± standard deviations (SD); (n=3).

3.8 In vitro lung Deposition Studies

Various critical aerodynamic parameters, such as mass median aerodynamic diameter (MMAD), percentage geometric standard deviation (%GSD), and percentage fine particle fraction (% FPF), were determined using the Anderson Cascade Impactor (ACI). The MMAD predicts the distribution of particles in the lungs. %GSD, on the other hand, measures the variability in particle diameter. GSDs below 1.2 are characteristic of monodisperse DPI systems. The fraction of the total inhaled dose reaching the value corresponding to the cutoff diameter of 5 µm is commonly referred to as the FPF.

The geometric mean diameter of the optimized MS3 microspheres was calculated from the volume-averaged surface diameter, and the theoretical MMAD was within the desired particle range of 2.12 ± 0.08 µm.

The optimized lyophilized microspheres MS3 had an MMAD of 2.4 ± 0.26 µm, which is close to the theoretical MMAD as well as % FPF and %GSD of 62 ± 0.41 and 0.8 ± 0.56, respectively, indicating a monodisperse system suitable for delivery to the depth of the lung. The MMAD value obtained for NRG SLN DOX sMS revealed an efficient deposition of the produced microspheres in the lungs, while a % GSD 0.8 indicated a uniform size distribution, ultimately promoting reproducible therapeutic activity.

3.9 *In vitro* Release Study

The developed microspheres loaded with NRG SLNR and DOX were subjected to an *in vitro* release study using simulated lung fluid (SLF) for 12 hours. The release of NRG and DOX showed an inhibitory pattern the higher the TPP concentration was (Table 6). These results are consistent with several previous findings (Cho et al., 2014; Desai and Park, 2015; Pai et al., 2016; Mulia et al., 2018), which reported that increasing TPP solution concentration results in an increase in matrix density, which in turn decreases drug release from chitosan-TPP microspheres. An Initial burst release (in the first 2 hours) was observed for the release of DOX from all formulations prepared, which agrees with earlier studies (Cho et al., 2014; Debnath et al., 2018).

[Please enter Table 6 here]

However, the release of NRG did not show a burst effect but a sustained release for up to 12 hours in all formulations prepared. Release studies have shown a rapid release of doxofylline with a sustained release of naringenin (Figure 10), resulting in the immediate treatment of asthma exacerbation by DOX followed by prolonged anti-inflammatory effect by naringenin, thus fulfilling the objective of this proposed new inhalable design approach. The release of DOX and NRG from the prepared swellable microspheres at 2, 6, and 12 hours is shown in Table 6.

[Please enter Figure 10 here]

Figure 10: *In vitro* drug release profiles of optimized microspheres, MS3 sMS. Abbreviations: DOX, Doxofylline; NRG, Naringenin; MS3 sMS, optimized microspheres formulation. The initial burst release of DOX was 50.5% at 2 h, followed by a constant release up to 8h. In the case of NRG, no burst release was observed in the first 2 h; while it depicted a sustained release of NRG throughout the study, the maximum NRG release was 72.3% within 12h. Values are represented as mean±standard deviation (SD) (n=3).

Drug release data were fitted to various release models such as zero-order, first-order, and Higuchi kinetics and analysed for linearity of the curves. In addition, the release data were fitted to the Korsmeyer-Peppas model, and the linearity and the release component “n” were determined. The results of the release kinetics are summarized in Table 7.

[Please enter Table 7 here]

The observed R^2 value of DOX release ranged from 0.904 to 0.961, 0.745 to 0.923, and 0.974 to 0.999 for zero-order, first-order, and Higuchi kinetics, respectively. The highest linearity was obtained with Higuchi kinetics and is consistent with previous studies (Cho et al., 2014; Ji et al., 2016). For NRG release, linearities of 0.963 to 0.995, 0.987 to 0.993, and 0.986 to 0.989 were observed for zero-order, first-order kinetics, and Higuchi, respectively. Moreover, the results were best fitted with Korsmeyer-Peppas with linearities of 0.965 to 0.996 and 0.991 to 0.995 for the release of DOX and NRG from the matrix, respectively. In the case of DOX release, the release component “n" values ranged from 0.46 to 0.52, indicating anomalous drug release for spherical matrices whose values ranged from 0.45 to 0.89. In addition, the value of "n" for NRG release from all formulations ranged from 0.71 to 0.81, which was also in a similar range of 0.45 to 0.89, implying that the release mechanisms of NRG and DOX followed more than one component, which could be a combination of erosion, dissolution, and diffusion from the swollen matrix (Cho et al., 2014; Debnath et al., 2018; Wang et al., 2021)
The *in vitro* release data indicated a rapid release of DOX and a sustained release of NRG from the developed microspheres.

- *Selection of optimized formulations for in-vivo studies*

In this study, the criteria for selecting the best formulations for *in vivo* studies were % EE, % DL, particle size, PDI, % swelling, and % drug release of DOX and NRG within 2 and 12 hours, respectively. The formulation MS3 with a chitosan/TPP ratio of 1:6 was found to have a mean particle size greater than 2 µm, a PDI of 0.310, a % EE of 79.5%, a % DL of 13.5%, a % swelling index greater than 80% in 2 hours, and a rapid release of DOX in the first 2 hours along with a sustained release of NRG up to 12 hours, thus meeting all desired criteria for effective targeted delivery to the lungs. Therefore, the MS3 microspheres loaded with NRG SLNs and DOX were used as an optimized formulation for further screening in the *in vivo* models.

3.10 In vivo Studies

The therapeutic efficacy of optimized inhalable swellable NRG SLNs and DOX-loaded microspheres was investigated in a murine asthma model using Albino mice(a combination of trypsin and egg albumin challenge-induced asthma). Both cause several clinical symptoms associated with bronchial asthma. These symptoms include antigen-induced bronchoconstriction, airway inflammation, bronchial eosinophilia, airway remodelling, and bronchial hyperresponsiveness.

3.10.1 Respiratory Rate, Tidal Volume, Airflow Rate

After the egg albumin challenge, there was a significant decrease ($p < 0.05$) in tidal volume and air flow rate in the asthmatic mice compared to the normal control mice (Table 8). In addition, the respiratory rate was significantly increased in the asthma group compared to the normal control group ($p < 0.05$). However, a significant increase ($p < 0.05$) in air flow rate and tidal volume was observed in the mice treated with dexamethasone and the optimized formulation compared to the asthmatic control group. In contrast, the respiratory rate was significantly decreased ($p < 0.05$) compared to the diseased animals of group II.

[Please enter Table 8 here]

3.10.2 Serum Bicarbonate

Serum bicarbonate levels were significantly elevated in asthmatic mice compared with normal mice. On day 35 of the study, serum bicarbonate levels were significantly ($p<0.05$) lower in the groups treated with the standard formulation ($p < 0.05$) and the optimized formulation ($p < 0.01$) compared to the asthmatic control group (Figure 11).

[Please enter Figure 11 here]

Figure 11: Effect of dexamethasone and optimized microspheres on serum bicarbonate levels. Values are represented as mean± standard error mean (n=6). Group I - normal control, Group II - asthmatic control, Group III – dexamethasone (5mg/kg), Group IV - formulation MS3. Significant difference versus group II: * $p < 0.05$, ** $p < 0.01$, *** $p < 0.001$; # $P<0.05$ versus normal control group. One-way ANOVA followed by post hoc Tukey's multiple range tests was performed.

3.10.3 Eosinophil Count

Asthma is characterised by an increased number of inflammatory cells, including eosinophils, neutrophils, and lymphocytes. Therefore, the number of eosinophils in the BAL fluid collected from mice lungs was determined (Figure 12).

When the animals were challenged with trypsin and egg albumin on the 35th day of the experiment, the mice in the asthmatic control group displayed a significantly higher eosinophil count than the normal control group ($p < 0.001$). In addition, eosinophils were significantly lower in mice treated with dexamethasone and optimized microspheres ($p < 0.001$).

Notably, eosinophils, the most common inflammatory cells in asthma, were significantly lower in mice treated with NRG SLNs and DOX-loaded microspheres. This finding suggests that administering NRG SLN DOX SMs to mice successfully reduced the number of inflammatory cells *in vivo*.

[Please enter Figure 12 here]

Figure 12: Eosinophil counts in BAL fluid after treatment with Dexamethasone and Microspheres. Values are represented as mean± standard error mean (n=6). Group I - normal control, Group II - asthmatic control, Group III – dexamethasone (5mg/kg), Group IV – optimized formulation, MS3. Significant difference versus group II: * $p < 0.05$, ** $p < 0.01$, *** $p < 0.001$; ### $P<0.001$ versus normal control group. One-way ANOVA followed by post hoc Tukey's multiple range tests was performed.

3.10.4 Histamine Release

Histamine levels were significantly higher in the asthmatic control group animals than in normal control animals ($p < 0.05$). Lower histamine levels ($p < 0.05$) were observed in animals treated with the optimized formulations than in the asthmatic control group (Figure 13).

[Please enter Figure 13 here]

Figure 13: Effect of optimized microspheres and dexamethasone on histamine concentration. Group I - normal control, Group II - asthmatic control, Group III – dexamethasone (5mg/kg), and Group IV – optimized formulation MS3. Values are represented as mean± standard error mean (n=6). Significant difference versus group II: * $p < 0.05$, ** $p < 0.01$, *** $p < 0.001$; ## $P<0.01$ versus normal control group. One-way ANOVA followed by post hoc Tukey's multiple range tests was performed.

3.10.5 Histopathology of Lungs

The results of the histopathological analyses are shown in Figure 14. While trypsin- and egg albumin-sensitized animals displayed severe inflammation and bronchial wall lining damage, the normal control mice exhibited healthy bronchial structures. Compared with the asthmatic control group, the mice treated with dexamethasone and the optimized formulation showed less bronchial wall damage, indicating a substantial response.

[Please enter Figure 14 here]

Figure 14: Histological examination of lung tissues. In the histological examination of lung tissue, hematoxylin dye was used to examine tissue morphology and lung inflammation levels in sections of

bronchus of A) asthmatic control mice, B) normal control mice, C) Dexamethasone treated mice, D) optimized microspheres, MS3 treated mice.

4. Conclusions

The present study demonstrated that inhalable, loosely cross-linked NRG SLNs and DOX-loaded swellable chitosan microspheres successfully delivered to the lungs, with an experimental MMAD of 2.4 µm and an FPF of about 62%. Glyceryl tristearate with soy lecithin can be used to formulate NRG SLNs, and among surfactants, Kolliphor® P188 showed the best results. Chitosan with the TPP cross-linking agent in the ratio of 1:6 showed the desired particle size, dispersity, entrapment efficiency, and drug loading. The swelling study also confirmed that the microspheres swelled to several times their size, which enabled them to avoid uptake by macrophages. NMR, FTIR, and XRD studies showed good carrier drug encapsulation and no interactions with the excipient. The *in vitro* drug release studies clearly indicated the rapid release of doxofylline with a percentage cumulative drug release of 50.5% in the first 2 hours and a sustained release of naringenin with a percentage drug release of 72.3 in 12 hours from the optimized NRG SLN DOX sMS. In addition, *in vivo* studies after six days of consecutive administration of the selected formulation showed a significant reduction in eosinophils in BAL fluid, serum bicarbonate levels, histamine release, and bronchial inflammation compared with asthmatic mice, and the results were significantly similar to those of normal mice. Bronchial hyperresponsiveness of microspheres-treated mice was significantly reduced compared with asthmatic mice. Histopathological examination also demonstrated the efficacy of the optimized inhalable microspheres, as no evidence of bronchial wall damage was observed. Thus, it can be concluded that this novel inhalable dual delivery system of DOX and NRG can be used as an excellent alternative to treat asthma effectively. Further pharmacokinetic studies are needed to investigate systemic and targeted drug delivery *in vivo*, and therapeutic efficacy can be tested in other animal models.

CRediT author statement

Ashutosh Pareek: Conceptualization, Methodology, Resources, Data Curation, Writing—Original Draft Preparation, Validation, Supervision, Project Administration, Methodology. **Rupal Kothari:** Methodology, Software, Investigation, Writing—Original Draft Preparation. **Aaushi Pareek:** Methodology, Software, Investigation, Writing—Original Draft Preparation, Validation. **Yashumati Ratan:** Writing-Reviewing and Editing, Formal Analysis, Validation. **Pushpa Kashania:** Formal Analysis, Investigation, Writing—Original Draft Preparation, Validation. **Vivek Jain:** Formal Analysis, Investigation, Writing—Original Draft Preparation, Validation. **Philippe Jeandet:** Data Curation, Writing- Reviewing And Editing, Validation. **Madan Mohan Gupta**: Software, Investigation, Writing- Reviewing And Editing, Data Curation. **Azmat Ali Khan**: Formal Analysis, Writing—Original Draft Preparation, Validation, Funding Acquisition. **Amer M. Alanazi**: Formal Analysis, Writing- Reviewing And Editing, Funding Acquisition.

Parveen Kumar: Investigation, Writing—Original Draft Preparation, Validation. All authors have read and agreed to the published version of the manuscript.

Funding

This work was funded by the Researchers Supporting Project Number (RSP2023R339) King Saud University, Riyadh, Saudi Arabia.

Institutional Review Board Statement

The animal study protocol was pre-approved by the Institutional Animal Ethical Committee of Banasthali Vidyapith, and all CPCSEA guidelines were followed for all experiments.

Acknowledgment

The authors are grateful to BanasthaliVidhyapith, Banasthali, India, for providing all the necessary resources for completing this report. The authors also thank Ritika Gurunani, Banasthali Vidyapith for technical support during animal experiments. The graphical abstract has been drawn using the biorender.com platform.

Declarations of interest: None.

References:

- Agnihotri, S.A., Mallikarjuna, N.N., Aminabhavi, T.M., 2004. Recent advances on chitosan-based micro-and nanoparticles in drug delivery. J Control Release. 100, 5–28.
- Ahmad, A., 2022. Pharmacological Strategies and Recent Advancement in Nano-Drug Delivery for Targeting Asthma. Life (Basel, Switzerland). 12, 596.
- Bernstein, D. I., 2008. ABCs of Asthma. Clin Cornerstone. 8, 9–25.
- Buzia, O.D., Dima, C., Dima, S., 2015. Preparation and characterization of chitosan microspheres for vancomycin delivery. Farmacia. 63, 897-902.
- Cais, M., 1961. The spectrofluorometric assay of serotonin and histamine in tissues following a common extraction procedure. Med Exp (Basel). 5, 73–76.
- Cazzola, M., Matera, M. G., 2020. The effect of doxofylline in asthma and COPD. Respir Med. 164(105904).
- Chen, S., Yang, X., Zhang, Y., Liu, Y., Lu, H., Qiu, Y., Cheng, L., Li, C., Wang, C., 2021. Inhalable Porous Microspheres Loaded with Metformin and Docosahexaenoic Acid Suppress Tumor Metastasis by Modulating Premetastatic Niche. Mol Pharmaceutics. 18, 2622–2633.
- Chen, Z., Chen, P., Wu, H., Shi, R., Su, W., Wang, Y., Li, P., 2020. Evaluation of Naringenin as a Promising Treatment Option for COPD Based on Literature Review and Network Pharmacology. Biomolecules. 10, 1644.
- Chin, L.H., Hon, C.M., Chellappan, D.K., Chellian, J., Madheswaran, T., Zeeshan, F., Awasthi, R., Aljabali, A.A., Tambuwala, M.M., Dureja, H., Negi, P., 2020. Molecular mechanisms of action of naringenin in chronic airway diseases. European journal of pharmacology. 879, 173139.
- Cho, A. R., Chun, Y. G., Kim, B. K., Park, D. J., 2014. Preparation of chitosan-TPP microspheres as resveratrol carriers. J Food Sci. 79, E568–E576.
- Chuacharoen, T., Prasongsuk, S., Sabliov, C. M., 2019. Effect of Surfactant Concentrations on Physicochemical Properties and Functionality of Curcumin Nanoemulsions Under Conditions Relevant to Commercial Utilization. Molecules (Basel). 24, 2744.
- Debnath, S.K., Saisivam, S., Debanth, M., Omri, A., 2018. Development and evaluation of Chitosan nanoparticles based dry powder inhalation formulations of Prothionamide. PLoS One. 13, e0190976.
- Desai, K.G.H., Park, H.J., 2005. Preparation and characterization of drug loaded chitosan–tripolyphosphate microspheres by spray drying. Drug Dev Res. 64,114–128.
- Dragostin, O.M., Tatia, R., Samal, S.K., Oancea, A., Zamfir, A.S., Dragostin, I., Lisa, E.L., Apetrei, C., Zamfir, C.L., 2020. Designing of Chitosan Derivatives Nanoparticles with Antiangiogenic Efect for Cancer Therapy. Nanomaterials (Basel). 10, 698.
- El-Sherbiny, I. M., McGill, S., Smyth, H. D., 2010. Swellable microparticles as carriers for sustained pulmonary drug delivery. J Pharm Sci. 99, 2343–2356.

- Feng, Y., Xia, W., 2011. Preparation, characterization and antibacterial activity of water-soluble O-fumaryl-chitosan. Carbohydr Polym . 83, 1169–1173.
- Gaspar, M. C., Sousa, J. J., Pais, A. A., Cardoso, O., Murtinho, D., Serra, M. E., Tewes, F., Olivier, J. C., 2015. Optimization of levofloxacin-loaded cross-linked chitosan microspheres for inhaled aerosol therapy. Eur J Pharm Biopharm. 96, 65–75.
- Glaab, T., Braun, A., 2021. Noninvasive Measurement of Pulmonary Function in Experimental Mouse Models of Airway Disease. Lung. 199, 255–261.
- Gohil, P., Thakkar, H., Gohil, U., Deshpande, S., 2011. Preliminary studies on the effect of rebamipide against the trypsin and egg-albumin induced experimental model of asthma. Acta Pharm. 61, 427–433.
- Gupta, K., Jabrail, F.H., 2006. Effects of degree of deacetylation and cross-linking on physical characteristics, swelling and release behavior of chitosan microspheres. CarbohydrPolym. 66, 43–54.
- Guttoff, M., Saberi, A. H., McClements, D. J., 2015. Formation of vitamin D nanoemulsion-based delivery systems by spontaneous emulsification: factors affecting particle size and stability. Food chemistry. 171, 117–122.
- Helgason, T., Awad, T.S., Kristbergsson, K., McClements, D.J., Weiss, J., 2009. Effect of surfactant surface coverage on formation of solid lipid nanoparticles (SLN). J Colloid Interface Sci. 334, 75-81.
- Ibrahim, M., Garcia-Contreras, L., 2013. Mechanisms of absorption and elimination of drugs administered by inhalation. Ther Deliv. 4, 1027–1045.
- Jasemi, S. V., Khazaei, H., Fakhri, S., Mohammadi-Noori, E., Farzaei, M. H., 2022. Naringenin Improves Ovalbumin-Induced Allergic Asthma in Rats through Antioxidant and Anti-Inflammatory Effects. Evidence-based complementary and alternative medicine. eCAM, 2022, 9110798.
- Ji, P., Yu, T., Liu, Y., Jiang, J., Xu, J., Zhao, Y., Hao, Y., Qiu, Y., Zhao, W., Wu, C., 2016. Naringenin-loaded solid lipid nanoparticles: preparation, controlled delivery, cellular uptake, and pulmonary pharmacokinetics. Drug Des Devel Ther. 10, 911–925.
- Kean, T., Thanou, M., 2010. Biodegradation, biodistribution and toxicity of chitosan. Adv Drug Deliv Rev. 62, 3–11.
- Kushwaha, A.K., Vuddanda, P.R., Karunanidhi, P., Singh, S.K., Singh, S., 2013. Development and evaluation of solid lipid nanoparticles of raloxifene hydrochloride for enhanced bioavailability. Biomed Res Int 2013, 584549.
- Li, J., Zheng, H., Qin, L., Xu, E. Y., Yang, L., Zhang, L., Zhang, X., Fan, L., Beck-Broichsitter, M., Muenster, U., Chen, L., Zhang, Y., Mao, S., 2019. *In vitro-In vivo* correlation of inhalable budesonide-loaded large porous particles for sustained treatment regimen of asthma. Acta Biomater. 96, 505–516.
- Li, N., Li, X., Cheng, P., Yang, P., Shi, P., Kong, L., Liu, H., 2021. Preparation of Curcumin Solid Lipid Nanoparticles Loaded with Flower-Shaped Lactose for Lung Inhalation and Preliminary Evaluation of Cytotoxicity *In vitro*. Evid Based Complement Alternat Med eCAM. 2021(4828169).
- Liang, Z., Nie, H., Xu, Y., Peng, J., Zeng, Y., Wei, Y., Wen, X., Qiu, J., Zhong, W., Deng, X., He, J., 2016. Therapeutic effects of rosmarinic acid on airway responses in a murine model of asthma. Int Immunopharmacol. 41, 90–97.

- Louie, S., Zeki, A. A., Schivo, M., Chan, A. L., Yoneda, K. Y., Avdalovic, M., Morrissey, B. M., Albertson, T. E., 2013. The asthma-chronic obstructive pulmonary disease overlap syndrome: pharmacotherapeutic considerations. Expert Rev Clin Pharmacol. 6, 197–219.
- Lupascu, F.G., Dash, M., Samal, S.K., Dubruel, P., Lupusoru, C.E., Lupusoru, R.V., Dragostin, O., Profire, L., 2015. Development, optimization and biological evaluation of chitosan scaffold formulations of new xanthine derivatives for treatment of type-2 diabetes mellitus. Eur. J. Pharm. Sci. 77, 122–134.
- Major-Godlewska, M., 2020. The influence of stirring time and frequency of impeller rotation on evaluation of drops dimensions and rheological properties of the multiple emulsion. Chem Pap. 74(9), 3135-3143.
- Moribe, H., Kitayama, Y., Suzuki, T., Okubo, M., 2012. Effect of stirring rate on particle formation in emulsifier-free, organotellurium-mediated living radical emulsion polymerization (emulsion TERP) of styrene. Polym J. 44, 205-210.
- Mulia, K., Andrie, Krisanti, E.A., 2018. Effect of sodium tripolyphosphate concentration and simulated gastrointestinal fluids on release profile of paracetamol from chitosan microsphere. *IOP Conf. Ser.: Mater Sci Eng*. 316, 012028.
- Müller, R.H., Radtke, M., Wissing, S.A., 2002. Solid lipid nanoparticles (SLN) and nanostructured lipid carriers (NLC) in cosmetic and dermatological preparations. Adv Drug Deliv Rev. 54(1), S131-S155.
- Oh, Y. J., Lee, J., Seo, J. Y., Rhim, T., Kim, S. H., Yoon, H. J., Lee, K. Y., 2011. Preparation of budesonide-loaded porous PLGA microparticles and their therapeutic efficacy in a murine asthma model. J Control Release. 150, 56–62.
- Oliveira, B., Santana, M. H. A., Ré, M. I., 2005. Spray-dried chitosan microspheres cross-linked with d, l-glyceraldehyde as a potential drug delivery system: preparation and characterization. Braz J Chem Eng. 22, 353-360.
- Pai, R. V., Jain, R. R., Bannalikar, A. S., Menon, M. D., 2016. Development and Evaluation of Chitosan Microparticles Based Dry Powder Inhalation Formulations of Rifampicin and Rifabutin. J Aerosol Med Pulm Drug Deliv. 29, 179–195.
- Pandita, D., Ahuja. A., Velpandian, T., Lather, V., Dutta, T., Khar, RK, 2009. Characterization and *In vitro* assessment of paclitaxel loaded lipid nanoparticles formulated using modified solvent injection technique. Pharmazie. 64, 301-310.
- Rehfeld, S. J., 1967. The effects of initial surfactant concentration and emulsification time upon the particle size and distribution of benzene-in-water emulsions. J Colloid Interface Sci. 24, 358-365.
- Riffo-Vasquez, Y., Venkatasamy, R., Page, C.P., 2018. Steroid sparing effects of doxofylline. Pulmonary Pharmacology & Therapeutics. 48,1-4.
- Rogliani, P., Calzetta, L., Or, J., Cazzola, M., Matera, M.G., 2019. Efficacy and safety profile of doxofylline compared to theophylline in asthma: a meta-analysis. Multidiscip Respir Med. 14.
- Satari, N., Taymouri, S., Varshosaz, J., Rostami, M., Mirian, M. 2020. Preparation and evaluation of inhalable dry powder containing glucosamine-conjugated gefitinib SLNs for lung cancer therapy. Drug Dev Ind Pharm. 46, 1265-1277.
- Shah, S. P., Gohil, P. V., Shah, G. B., 2010. Role of estrogen receptor- α in an experimental model of bronchial asthma. Iran Biomed J. 14, 41–48.

- Steiner, D., Bunjes, H., 2021. Influence of process and formulation parameters on the preparation of solid lipid nanoparticles by dual centrifugation. Int J Pharm X. 3, 100085.
- Thatipamula, R., Palem, C., Gannu, R., Mudragada, S., Yamsani, M., 2011. Formulation and *In vitro* characterization of domperidone loaded solid lipid nanoparticles and nanostructured lipid carriers. Daru. 19, 23-32.
- Wang, L., Wang, X., Shen, L., Alrobaian, M., Panda, S. K., Almasmoum, H. A., Ghaith, M.M., Almaimani, R.A., Ibrahim, I.A.A., Singh, T., Baothman, A.A., Choudhry, H., Beg, S. 2021. Paclitaxel and naringenin-loaded solid lipid nanoparticles surface modified with cyclic peptides with improved tumor targeting ability in glioblastoma multiforme. Biomed Pharmacother. 138, 111461.
- Xue, N., Wu, X., Wu, L., Li, L., Wang, F., 2019. Antinociceptive and anti-inflammatory effect of Naringenin in different nociceptive and inflammatory mice models. Life sciences. 217, 148-154.
- Yuan, Y. Q., Zou, X. W., Xiong, P. F., 2003. Effects of temperature on the emulsification in surfactant-water-oil systems. Int J Mod Phys B. 17, 2773-2780.
- Zhang, L., Yang, L., Zhang, X., Jiaqi, L., Fan, L., Beck-Broichsitter, M., Zhang, X., Muenster, U., Wang, X., Zhao, J., Zhang, Y., Mao, S., 2018. Sustained therapeutic efficacy of budesonide-loaded chitosan swellable microparticles after lung delivery: Influence of *In vitro* release, treatment interval and dose. J Control Release. 283, 163–174.

Figure Captions

Figure 1: Graphical representation of a) Particle size and polydispersity index of optimized SLNs; formulation F6 contains 0.75% P188 b) Zeta potential of optimized SLNs; formulation F6 contains 0.75% P188. Abbreviations: SLNs, solid lipid nanoparticles; P188, Kolliphor P188.

Figure 2: Transmission electron microscopic image of optimized SLNs, formulation F6 contains 0.75% P188. Abbreviations: SLNs, solid lipid nanoparticles; P188, Kolliphor P188.

Figure 3: Graphical representation of a) the particle size of optimized microspheres, MS3 b) the Zeta potential of the optimized microspheres, MS3.

Figure 4: Scanning electron microscopic images of optimized NRG SLNs and DOX-loaded microspheres. Abbreviations: NRG SLNs, Naringenin-loaded solid lipid nanoparticles; DOX, Doxofylline.

Figure 5: Atomic force microscopic images of the optimized microspheres, MS3.

Figure 6: X-ray diffraction (XRD) graphs of NRG, DOX, NRG SLNs, Dummy SLNs, Dummy sMS and NRG SLN DOX sMS. Abbreviations: NRG, Naringenin; DOX, Doxofylline; NRG SLNs, Naringenin loaded solid lipid nanoparticles; Dummy SLNs, Dummy solid lipid nanoparticles; Dummy sMS, Dummy microspheres; NRG SLN DOX sMS, Naringenin solid lipid nanoparticles and Doxofylline co-loaded microspheres.

Figure 7: FTIR characterization spectra of (A) NRG, Physical Mixture, Excipients, Dummy and Drug Loaded SLNs (B) DOX, Physical Mixture, Excipient, Dummy and Drug loaded sMS. Abbreviations: FTIR, Fourier transform infrared spectroscopy; NRG, Naringenin; DOX, Doxofylline; SLNs, Solid lipid nanoparticles; sMS, Microspheres.

Figure 8: Nuclear magnetic resonance characterization spectra of A) NRG B) Dummy SLNs C) NRG-loaded SLNs D) DOX E) Dummy sMS F) NRG SLN DOX sMS. Abbreviations: NRG, Naringenin; Dummy SLNs, Dummy solid lipid nanoparticles; NRG SLNs,- Naringenin-loaded solid lipid nanoparticles; DOX, Doxofylline; Dummy sMS, Dummy microspheres; NRG SLN DOX sMS, Naringenin solid lipid nanoparticles and Doxofylline co-loaded microspheres.

Figure 9: Comparative graphical representation of the swelling Indexes of different formulations of microspheres. Values are represented as mean ± standard deviations (SD) (n=3).

Figure 10: *In vitro* drug release profiles of optimized microspheres, MS3 sMS. Abbreviations: DOX, Doxofylline; NRG, Naringenin; MS3 sMS, optimized microspheres formulation. The initial burst release of DOX was 50.5% at 2 h, followed by a constant release up to 8h. In the case of NRG, no burst release was observed in the first 2 h; while it depicted a sustained release of NRG throughout the study, the maximum NRG release was 72.3% within 12h. Values are represented as mean±standard deviation (SD) (n=3).

Figure 11: Effect of dexamethasone and optimized microspheres on serum bicarbonate levels. Values are represented as mean± standard error mean (n=6). Group I - normal control, Group II - asthmatic control, Group III – dexamethasone (5mg/kg), Group IV - formulation MS3. Significant difference versus group II: * $p < 0.05$, ** $p < 0.01$, *** $p < 0.001$; # $P<0.05$ versus normal control group. One-way ANOVA followed by post hoc Tukey's multiple range tests was performed.

Figure 12: Eosinophil counts in BAL fluid after treatment with Dexamethasone and Microspheres. Values are represented as mean± standard error mean (n=6). Group I - normal control, Group II - asthmatic control, Group III – dexamethasone (5mg/kg), Group IV – optimized formulation, MS3. Significant difference versus group II: * $p < 0.05$, ** $p < 0.01$, *** $p < 0.001$; ### $P<0.001$ versus normal control group. One-way ANOVA followed by post hoc Tukey's multiple range tests was performed.

Figure 13: Effect of optimized microspheres and dexamethasone on histamine concentration. Group I - normal control, Group II - asthmatic control, Group III – dexamethasone (5mg/kg), and Group IV – optimized formulation MS3. Values are represented as mean± standard error mean (n=6). Significant difference versus group II: * $p < 0.05$, ** $p < 0.01$, *** $p < 0.001$; ## $P<0.01$ versus normal control group. One-way ANOVA followed by post hoc Tukey's multiple range tests was performed.

Figure 14: Histological examination of lung tissues. In the histological examination of lung tissue, hematoxylin dye was used to examine tissue morphology and lung inflammation levels in sections of bronchus of A) asthmatic control mice, B) normal control mice, C) Dexamethasone treated mice, D) optimized microspheres, MS3 treated mice.

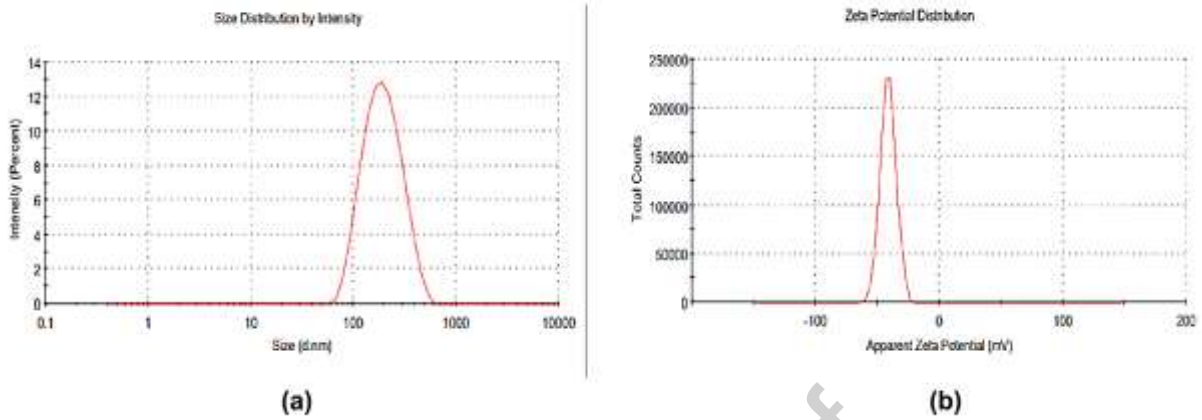

Figure 1

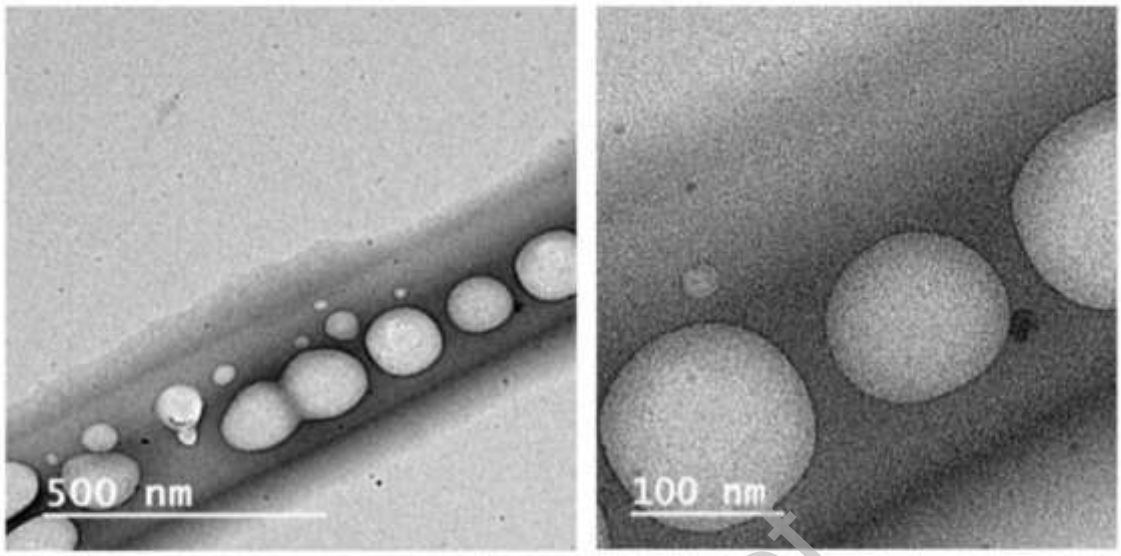

Figure 2

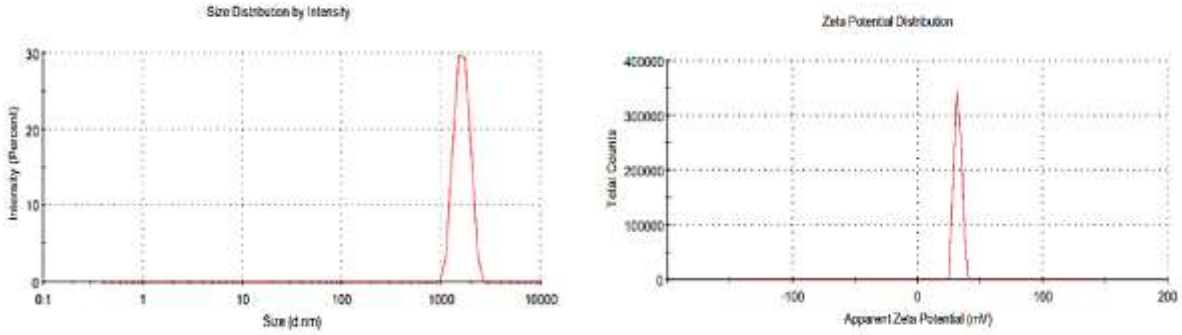

(a) (b)

Figure 3

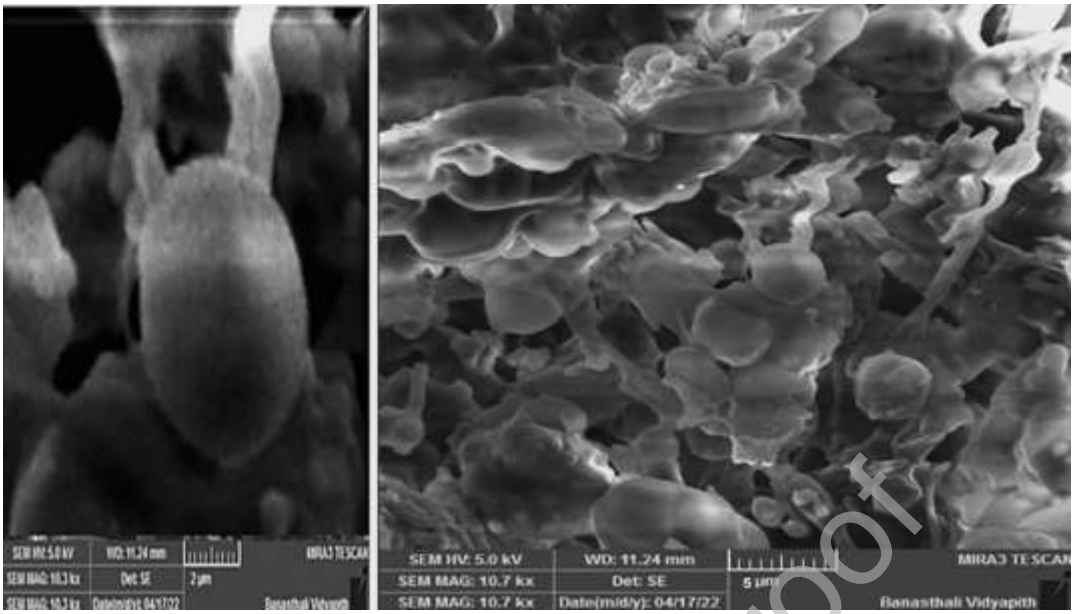

Figure 4

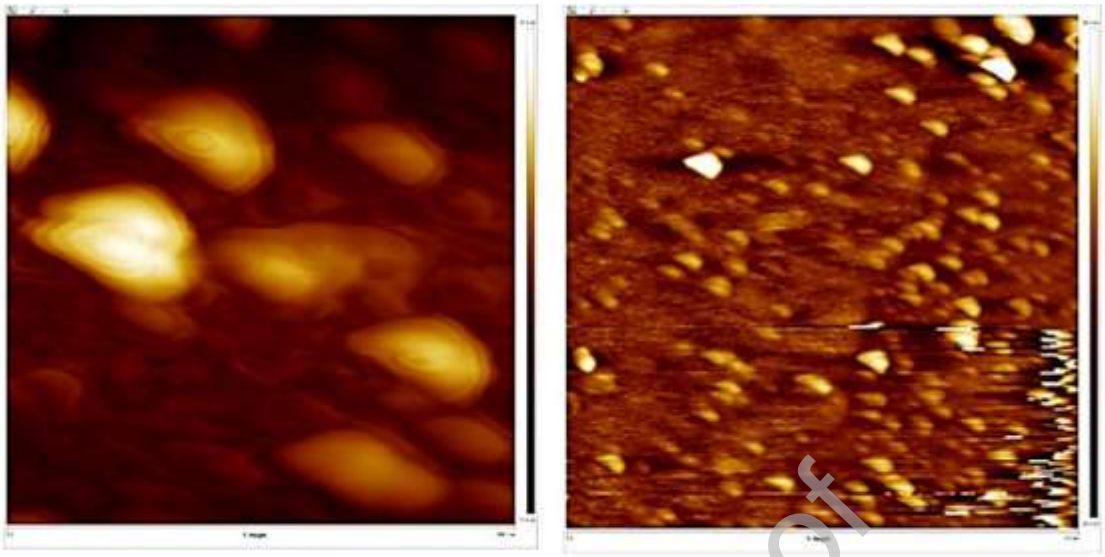

Figure 5

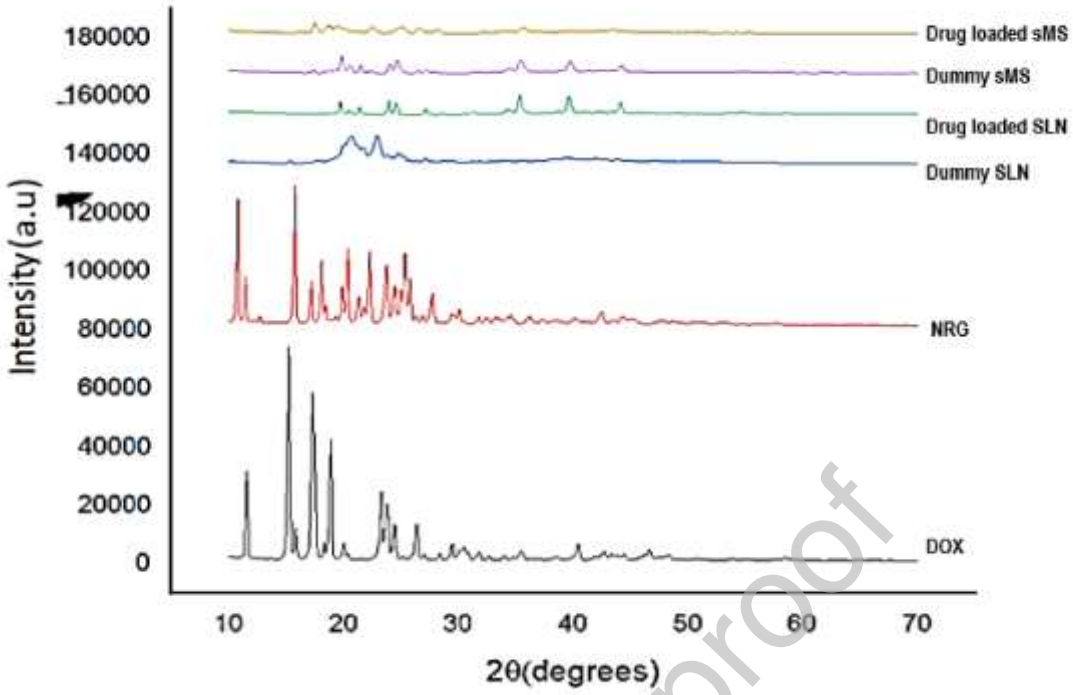

Figure 6

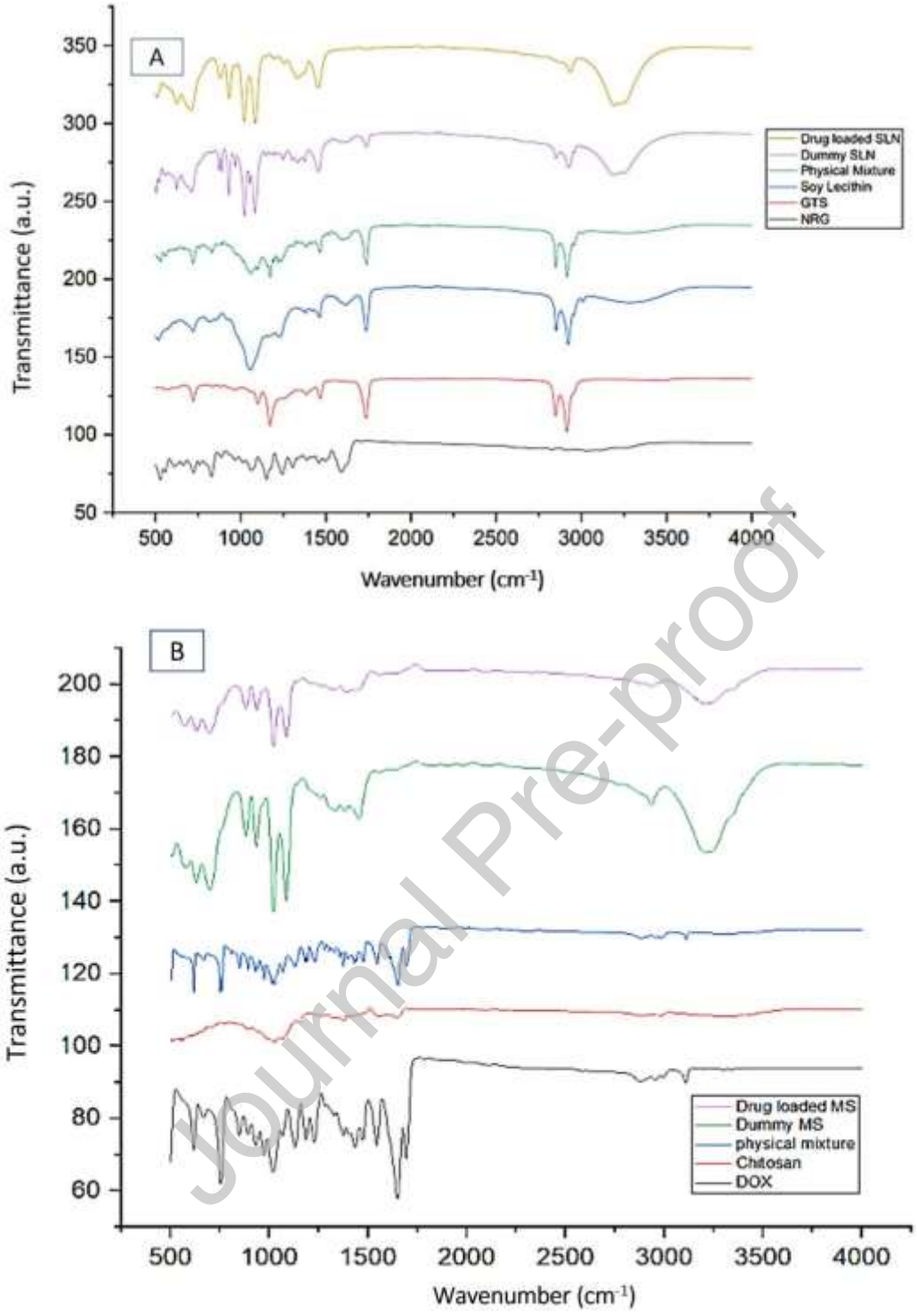

Figure 7

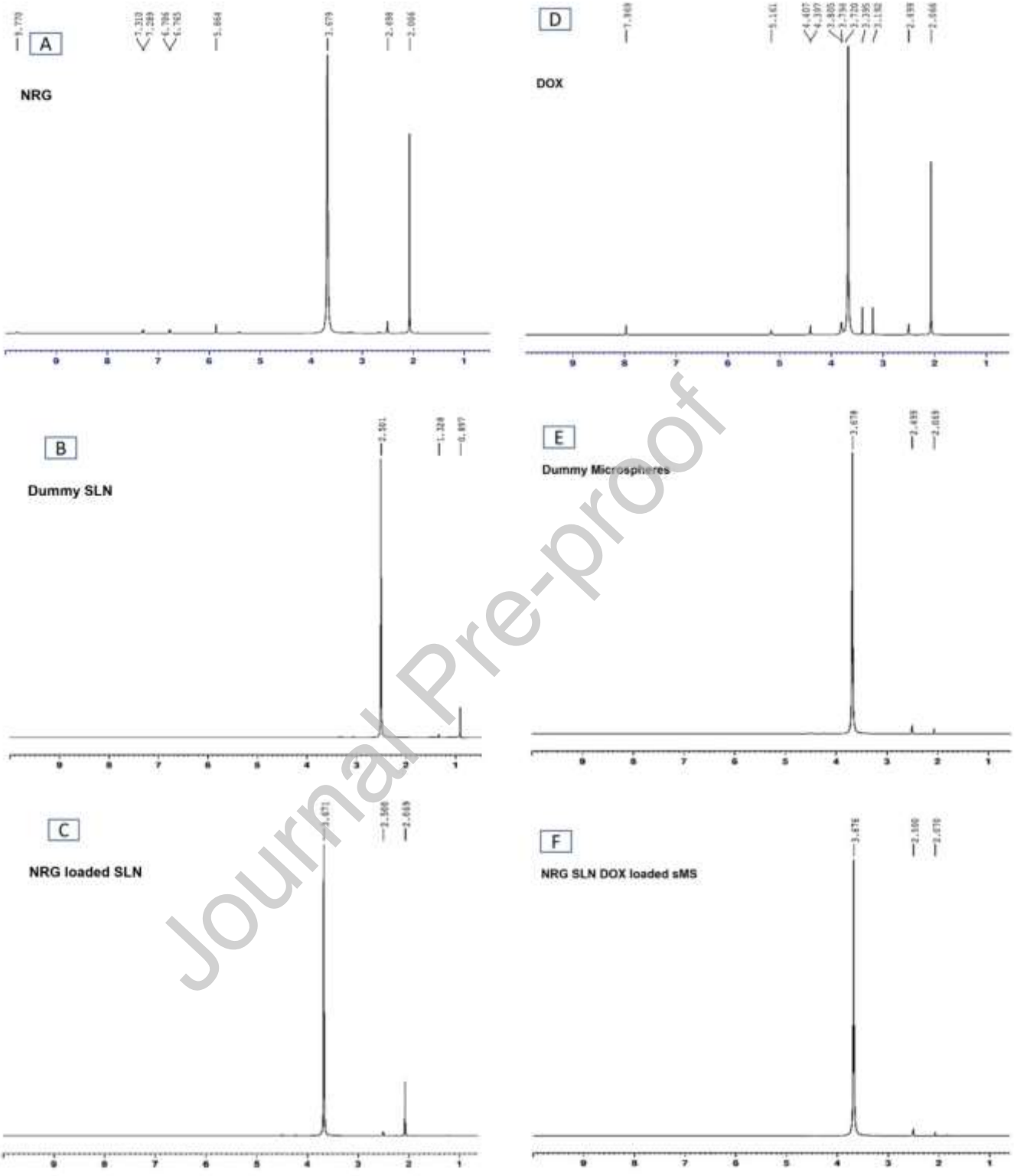

Figure 8

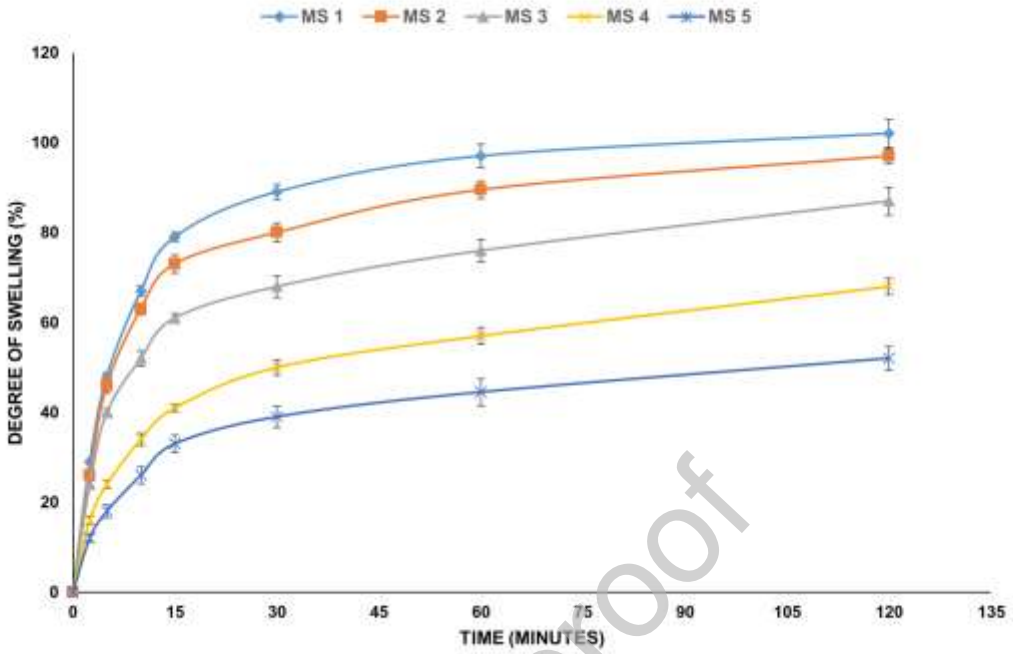

Figure 9

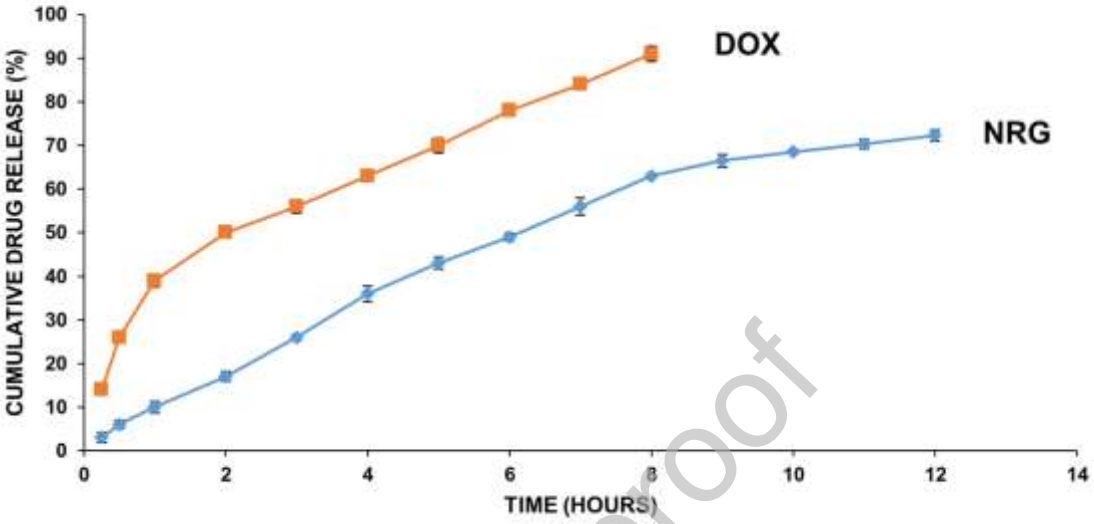

Figure 10

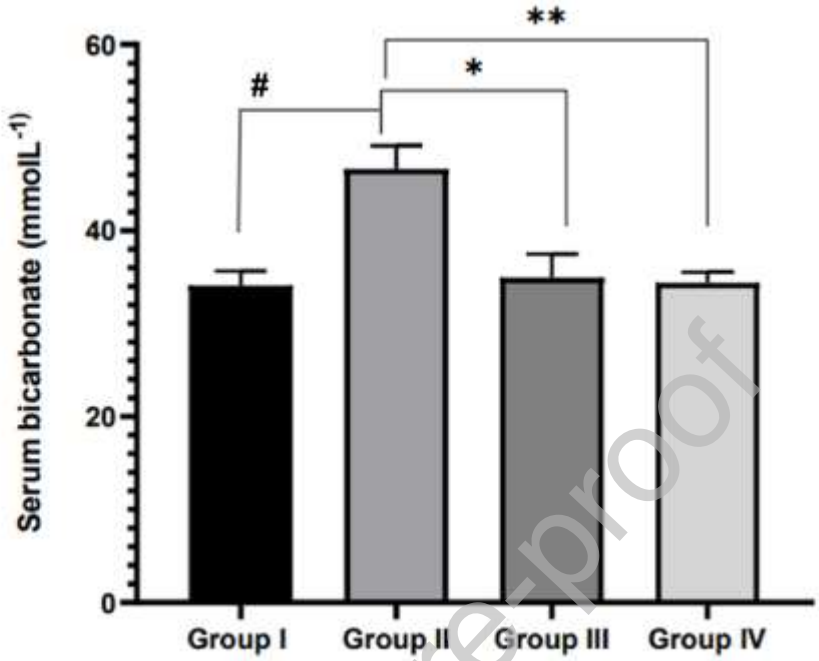

Figure 11

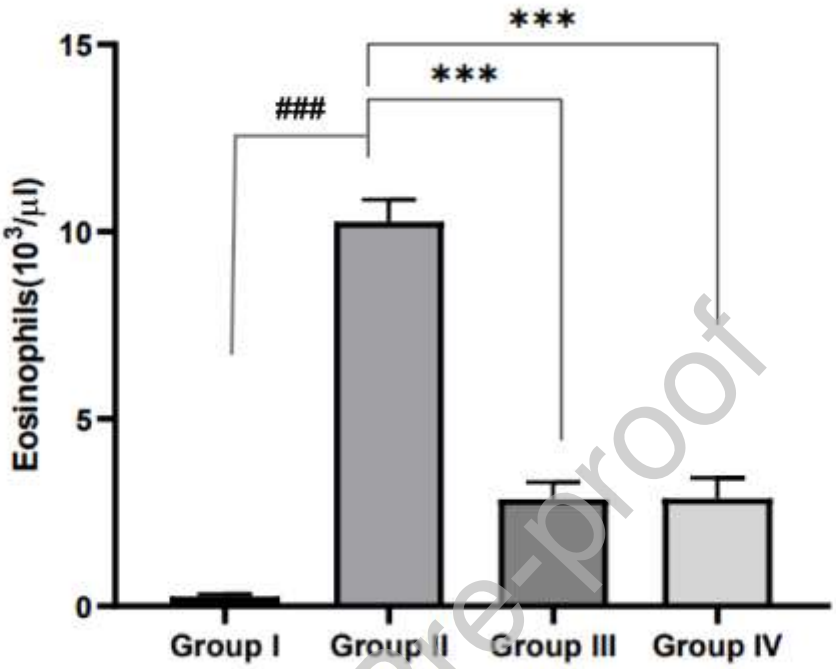

Figure 12

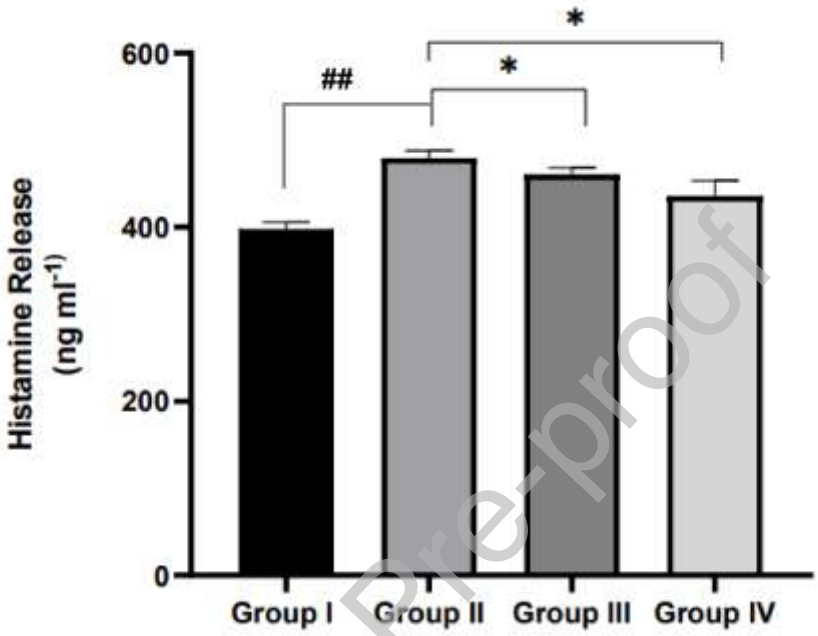

Figure 13

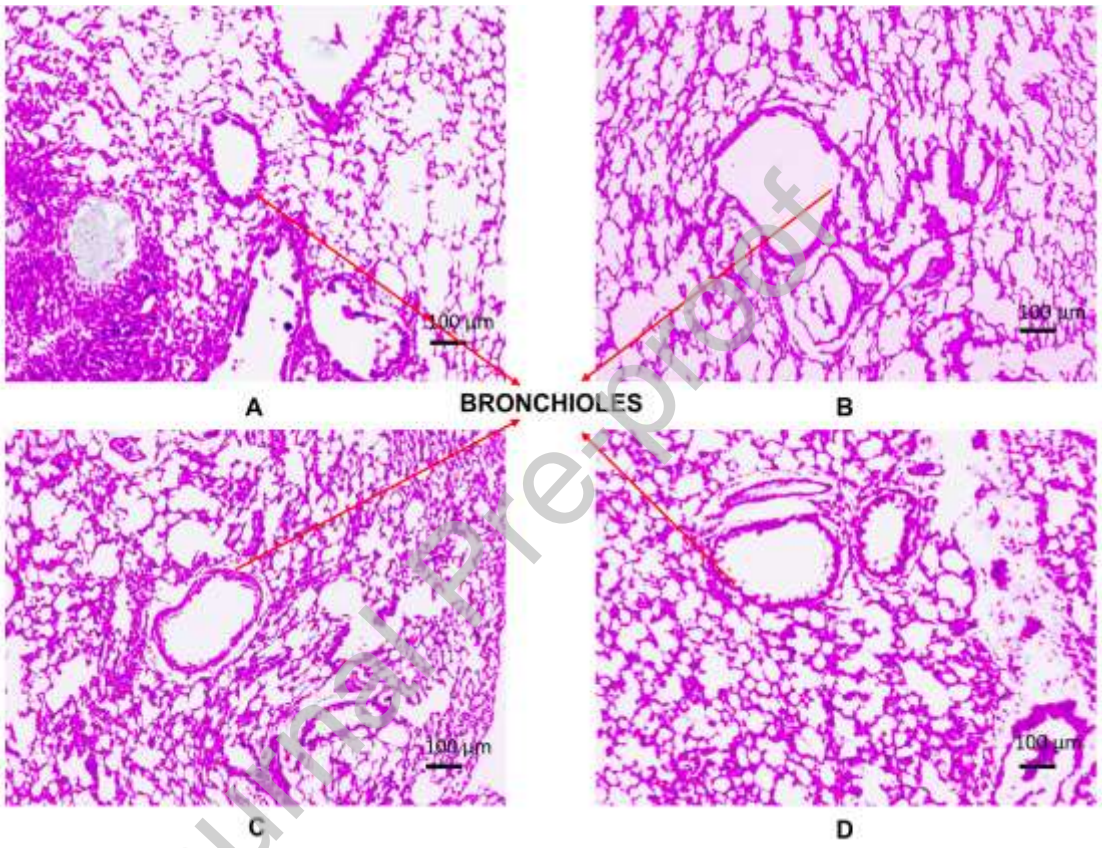

Figure 14

Table Captions

Table 1. Effect of stirring speed on particle size, zeta potential, and entrapment efficiency (EE%).

Table 2. Effect of varying temperatures on particle size, PDI, and Zeta Potential.

Table 3. Effect of Stirring Time on Particle Size, PDI, and Zeta Potential.

Table 4. Influence of surfactant concentration on particle size, PDI, Zeta potential, % EE and % DL while keeping process parameters constant.

Table 5. Particle size, PDI, zeta potential, % EE and %DL of NRG SLNs and DOX-loaded microspheres.

Table 6. *In vitro* drug release data of NRG SLNs and DOX-loaded microspheres.

Table 7. *In vitro* Drug release kinetics data of the different formulations.

Table 8. The therapeutic effect of dexamethasone and optimized microspheres on lung function parameters.

Table 1. Effect of stirring speed on particle size, zeta potential, and entrapment efficiency (EE%).

Stirring speed	Particle size (nm)	PDI	Zeta potential (mV)	EE (%)
300	321±3.1	0.654	-35.9±0.8	67.5±1.2
700	268±2.7	0.414	-34.7±0.4	79.9±0.9
1100	198±2.1	0.298	-33.9±0.6	93.2±1.6
1500	233±3.1	0.561	-34.8±0.7	76.5±1.2
1900	255±2.4	0.761	-33.1±0.6	70.5±2.3

Abbreviations: PDI, Polydispersity Index; E.E., Entrapment efficiency
Values are represented as mean±standard deviation (SD); (n=3).

Table 2. Effect of varying temperatures on particle size, PDI, and Zeta Potential.

Temperature (°C)	Particle size (nm)	PDI	Zeta potential (mV)	EE (%)
60	516±3.8	0.615	-35.9±0.7	89.2±1.7
70	303±2.4	0.513	-34.3±1.1	88.9±2.3
80	179±1.7	0.234	-34.9±0.5	92.7±2.1
90	172±2.3	0.467	-29.1±0.6	77.2±1.9
100	169±2.1	0.615	-29.9±0.4	71.9±1.4

Abbreviations: PDI, Polydispersity Index; E.E., Entrapment efficiency
Values are represented as mean± standard deviation (SD); (n=3).

Table 3. Effect of Stirring Time on Particle Size, PDI, and Zeta Potential.

Stirring time (hrs)	Particle size (nm)	PDI	Zeta potential (mV)	EE(%)
1	514±4.3	0.561	-35.9±0.4	78.1±1.3
2	191±1.9	0.211	-34.1±0.3	91.6±1.7
3	198±2.1	0.261	-33.2±0.4	87.7±1.5
4	187±2.6	0.259	-32.1±0.2	86.9±1.4
5	179±1.5	0.359	-31.9±0.4	82.8±1.9

Abbreviations: PDI, Polydispersity Index; E.E., Entrapment efficiency
Values are represented as mean±standard deviation (SD); (n=3).

Table 4. Influence of surfactant concentration on particle size, PDI, Zeta potential, % EE and % DL while keeping process parameters constant.

Code	Formulation	Particle size (nm)	PDI	Zeta potential (mV)	EE (%)	DL (%)
F1	0.5% P407	429.2±2.9	0.341	-21.8±1.7	82.7±1.6	11.5±0.7
F2	0.75% P407	218.7±1.7	0.284	-32.4±0.9	88.8±1.4	14.8±0.9
F3	1.0% P407	178.9±1.9	0.215	-36.4±0.4	90.0±0.7	17.6±1.1
F4	1.25% P407	189.2±2.4	0.186	-41.8±0.3	92.1±1.1	17.2±0.6
F5	0.5% P188	311.2±3.1	0.303	-42.2±0.9	85.3±2.1	14.7±0.7
F6	0.75% P188	159.8±1.8	0.172	-42.9±0.6	95.4±1.3	19.4±1.2
F7	1.0% P188	157.2±2.4	0.181	-45.1±0.3	95.5±1.4	17.8±0.6
F8	1.25% P188	168.4±2.7	0.184	-45.6±0.6	92.9±1.7	15.8±0.4

Abbreviations: PDI, Polydispersity Index; E.E., Entrapment efficiency; DL, Drug Loading
Values are represented as mean±standard deviation (SD); (n=3).

Table 5. Particle size, PDI, zeta potential, % EE and %DL of NRG SLNs and DOX-loaded microspheres.

Code	Chitosan:TPP Ratio	Mean Particle size (µm)	PDI	Zeta potential (mV)	EE (%)	DL (%)
MS1	1:2	0.59±0.09	0.561	34.1±1.2	85.4±1.7	17.4±1.7
MS2	1:4	1.05±0.12	0.441	32.4±0.7	81.7±2.0	14.7±1.1
MS3	1:6	2.09±0.08	0.310	31.2±0.9	79.5±1.4	13.5±0.9
MS4	1:8	2.18±0.14	0.318	30.2±0.5	67.8±1.6	12.1±1.1
MS5	1:10	2.41±0.18	0.516	29.1±1.1	63.6±2.1	10.8±0.9

Abbreviations: PDI, Polydispersity Index; EE, Entrapment efficiency; DL, Drug Loading and NRG SLNs-Naringenin loaded solid lipid nanoparticles
Values are represented as mean±standard deviation (SD); (n=3).

Table 6. *In vitro* drug release data of NRG SLNs and DOX-loaded microspheres.

	Cumulative drug release (%)					
Time	At 2 hours		At 6 hours		At 12 hours	
Code	DOX	NRG	DOX	NRG	DOX	NRG
MS1	64.2±1.3	21.7±0.7	91.5±1.4	57.6±1.2	--	84±1.2
MS2	54.4±1.1	20.2±0.7	84.5±1.2	56.2±1.1	--	81.6±1.4
MS3	50.5±1.2	17.6±1.1	78.1±1.3	49.4±0.9	--	72.3±1.3
MS4	44.6±0.9	14.5±0.9	74.9±0.9	45.3±0.7	--	67±1.1
MS5	39.3±0.8	14.3±1.0	69.5±1.1	42.7±0.8	98±1.6	59.5±0.9

Abbreviations: NRG SLNs- Naringenin loaded solid lipid nanoparticles; DOX- Doxofylline and NRG- Naringenin; Values are represented as mean±standard deviation (SD); (n=3).

Table 7. *In vitro* Drug release kinetics data of the different formulations.

Model	Zero-order		First order		Higuchi		Korsmeyer-Peppas			
Compo-nent	R^2		R^2		R^2		R^2		N	
Code	DOX	NRG	DOX	NRG	DOX	NRG	DOX	NRG	DOX	NRG
MS1	0.904	0.995	0.871	0.993	0.974	0.989	0.965	0.995	0.46	0.71
MS2	0.904	0.976	0.745	0.994	0.986	0.990	0.975	0.996	0.47	0.73
MS3	0.904	0.963	0.923	0.993	0.987	0.986	0.976	0.995	0.49	0.82
MS4	0.963	0.966	0.835	0.993	0.999	0.986	0.994	0.992	0.51	0.83
MS5	0.960	0.960	0.904	0.987	0.999	0.988	0.996	0.992	0.52	0.87

Abbreviations: DOX, Doxofylline; NRG, Naringenin; All the values are represented as the mean of 3 observations

Table 8. The therapeutic effect of dexamethasone and optimized microspheres on lung function parameters.

Parameter	Group I	Group II	Group III	Group IV
Respiratory rate (breaths per min)	180.62 ± 4.4	230.71 ± 1.54 [a]	179.84± 4.20 *	180.73± 5.98 *
Air flow rate (ml min-1)	13.26± 0.35	2.09± 0.11[a]	9.25± 0.48 *	9.62± 0.77 *
Tidal volume (ml)	0.09± 0.04	0.04± 0.01[a]	0.07± 0.01*	0.07± 0.01 *

Values represented as mean± standard error mean (n=6); P<0.05 versus the normal control group, *P<0.05 versus the asthmatic control group. Group I - normal control, Group II - asthmatic control, Group III – dexamethasone, and Group IV - Formulation MS3.

Graphical abstract